1

Fundamentals of Acoustic Wave Generation and Propagation

Mehmet A. Sahin[1], Mushtaq Ali[2], Jinsoo Park[2], and Ghulam Destgeer[1]

[1] Technical University of Munich, Central Institute for Translational Cancer Research (TranslaTUM), Control and Manipulation of Microscale Living Objects, School of Computation, Information and Technology (CIT), Department of Electrical Engineering, Einsteinstraße 25, Munich 81675, Germany
[2] Chonnam National University, Multiscale Flow Control Laboratory, Department of Mechanical Engineering, Gwangju 61186, Republic of Korea

1.1 Introduction

1.1.1 Acoustic or Sound Waves

The use of acoustic technologies is widespread, from radio frequency (RF) surface acoustic wave (SAW) filters in most telecommunication devices and nondestructive testing (NDT) of solid parts in expensive machineries to ultrasonic imaging of fetuses during pregnancy and of joints and bones in case of injuries. At the heart of any acoustic technology are sound waves at work – a combination of pressure and velocity fluctuations propagating through a medium. The terms "acoustic" or "sound" waves are interchangeably used. Since "sound" is commonly associated with hearing audible acoustic waves as perceived by the human auditory organs, it would be restrictive to limit the term sound to human perception only, the audible frequency range of 20 Hz to 20 kHz (Figure 1.1). Dogs and cats can even hear much higher-frequency ultrasound waves, whereas elephants via their feet can sense very low-frequency seismic vibrations propagating long distances across the land, i.e. infrasound. The ability of whales and bats to echolocate their targets at much higher frequencies of up to 200 kHz is also well known. Moreover, the use of MHz frequency waves in NDT and GHz frequency waves in SAW filters further broadens the scope of sound/acoustic waves. Therefore, any periodic pressure/velocity fluctuation in a solid, liquid, or gaseous media over a wide range of frequencies (10^0–10^9 Hz) can be safely called a sound/acoustic wave [1].

1.1.2 Dominos Effect

In an acoustic wave, the localized pressure at any given point within the medium oscillates between the maximum and minimum pressure values, linked to regions

Acoustic Technologies in Biology and Medicine, First Edition.
Edited by Adem Ozcelik, Ryan Becker, and Tony Jun Huang.

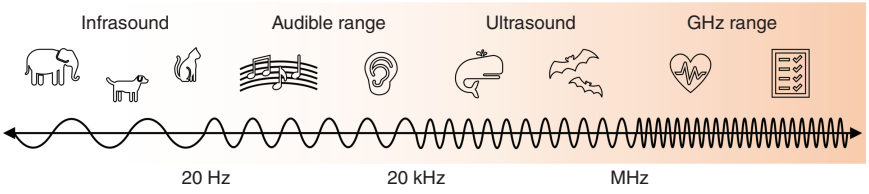

Figure 1.1 Categorization of acoustic waves based on frequency range.

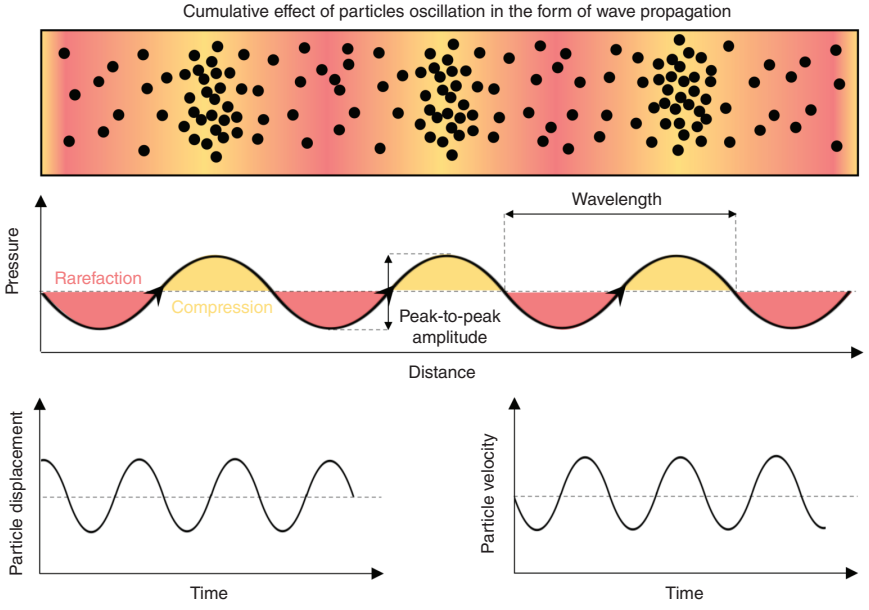

Figure 1.2 Particle oscillation in a medium because of an acoustic wave propagation.

of compression and rarefaction, respectively (Figure 1.2). Any particle of the discretized medium, without moving along the propagating wave, will vibrate about a mean position with an oscillating velocity field. Propagation of an acoustic wave with these oscillating pressure and velocity fields through a medium can be understood by a simple analogy of a stack of falling dominoes, where the disturbance originating from one end of the dominoes' stack reaches the opposite end in no time, even without a single domino piece significantly moving away from its original position. Here, the average velocity of an individual domino is related to the particle velocity of the medium, whereas the disturbance moving across the stack is analogous to wave propagation. It is important to distinguish the oscillating particle velocity from the velocity of wave propagation [2].

1.1.3 Elastic vs Inelastic Waves

Acoustic waves under discussion are broadly categorized as elastic waves since they need an elastic medium to propagate. For an acoustic wave propagation, as the particles of the elastic medium move about an equilibrium position, the velocity of

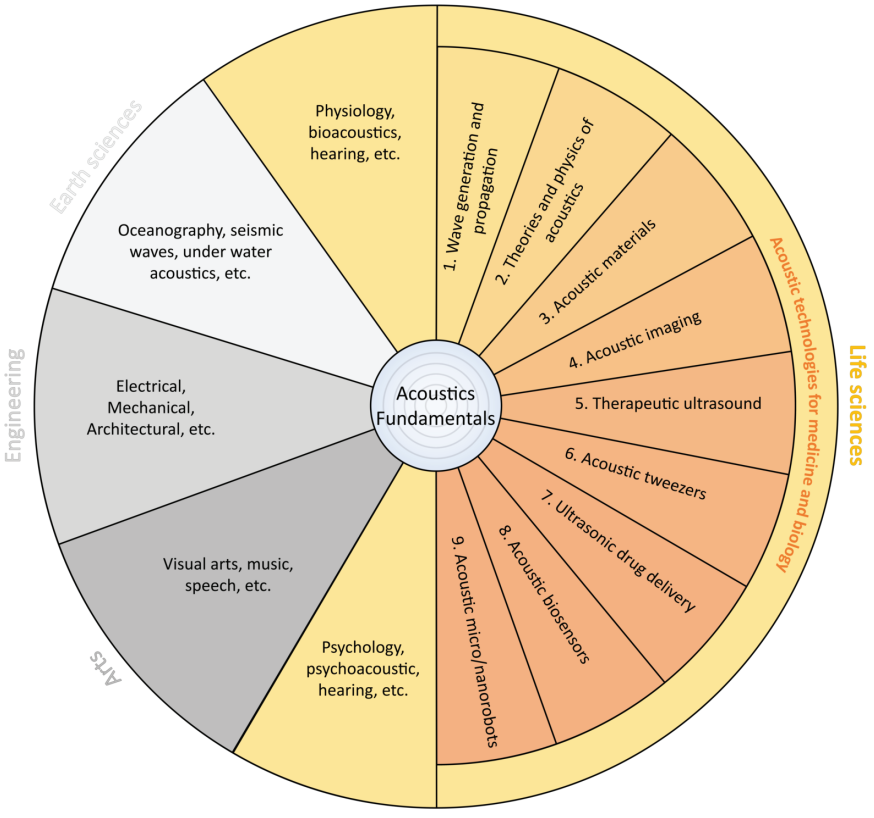

Figure 1.3 Position of "acoustic technologies for medicine and biology" within the scope of acoustics plotted in a circular chart analogous to Lindsay's wheel. Source: Adapted from Lindsay [5].

these particles determines the kinetic energy, whereas the displacement away from the equilibrium position (i.e. wave amplitude) determines the potential energy associated with the acoustic wave. Similarly, mechanical waves, e.g. a transverse wave visualized on a vibrating string, require a medium to propagate that can store kinetic and potential energies. Elastic waves also share a lot in terms of wave propagation and energy with electromagnetic waves that can even travel through vacuum and have an enormous frequency range: 10–10^6 Hz radio waves, 10^{14} Hz visible light, 10^{20} Hz gamma rays, etc. Since vacuum can store electric and magnetic energies, analogous to potential and kinetic energies in elastic waves, it can sustain electromagnetic waves propagation. Electromagnetic waves (e.g. visible light) can also propagate through medium other than vacuum; however, the waves will be subjected to phenomena like reflection and refraction at interfaces where electromagnetic properties of media (e.g. refractive index) change. Similarly, acoustic waves can be reflected and refracted at an interface where the wave propagation velocity or acoustic impedance is not continuous. Building upon the fundamental assumptions of geometrical optics, where a wave can be represented

by a ray directed normal to the wavefront, the paths taken by an acoustic wave in a complex medium can be described by Snell's law [3, 4].

1.1.4 Scope of Acoustics

The scope and ramifications of acoustics span across disciplines, i.e. from arts and engineering to earth and life sciences, where the boundaries separating them are not strictly defined (Figure 1.3). For example, acoustics of large spaces are closely linked to architectural engineering and have deep connections with how visual art is perceived in a theater. Details on the underlying acoustic connection between different disciplines can be found elsewhere [2]. Here, we will focus mainly on the role of acoustics and its applications within life sciences. Inspired by Lindsay's wheel [5], Figure 1.3 briefly indicates how acoustics, with its fundamental concepts at the center, is associated with various disciplines, including the topic of "acoustic technologies for medicine and biology" with additional subtopics (1–9) under the umbrella of life sciences. The subtopics are analogous to the chapters of this book, starting with the first chapter "Fundamentals of Acoustic Wave Generation and Propagation" followed by the rest as indicated in Figure 1.3.

1.2 Brief History of Acoustic Waves

1.2.1 Early History

In the sixth century BCE, Pythagoras discovered the relationship between the length of the vibrating strings and the variable-pitch musical sounds they produced. More than two millennia later, in 1643, Torricelli demonstrated that sound does not propagate in vacuum, thus establishing the need for media for sound propagation. Half a century later, in 1701, Sauveur introduced the term "acoustics" to describe the science of "sound," thereby pitching the two terms as synonyms to each other. A century later, in 1802, Chladni brought acoustics to the spotlight by introducing it as a separate branch of physics. With the development of acoustic resonators in 1859, also known as Helmholtz resonators, which are based on resonance of sound waves within a cavity, acoustics principles later found their applications in sound amplification or silencing in loudspeakers or mufflers, respectively. In 1866, Kundt measured the speed of sound propagating through a tube filled with fine powder to trace the acoustic pressure nodes of standing waves. As the classical acoustics matured by the end of the nineteenth century, Rayleigh culminated the state of the art of that time in his book *The Theory of Sound* (1896), which is still relevant today [2, 6, 7].

1.2.2 History of Acoustic Streaming

A historical advancement of acoustics can be further traced at multiple fronts; however, for the sake of brevity, we will only focus on the development of the following two topics: acoustic streaming flow and acoustic radiation force (ARF). Lord Rayleigh (1884), while explaining observations done by Faraday (patterns

on vibrating Chladni plates) [8] and Dvorak (circulation of air in Kundt's tubes experiment), [9] described a "boundary layer driven" flow within the context of standing wave resonators with mean fluid motion outside of the boundary layer, also known as "outer streaming" or "Rayleigh streaming" [10]. A mean flow within the boundary layer is called "Schlichting streaming" after Schlichting provided detailed analysis of this secondary flow within an incompressible boundary layer [11]. Contrary to a standing wave, a progressive or traveling wave dissipating acoustic energy within a viscous media along its path results in a time-averaged flow field in the form of "quartz wind" or "Eckart streaming," first described by Eckart [12]. With the advent of SAW technology (1965), it became possible to produce high-frequency (>10 MHz) acoustic waves in an efficient manner [13]. Shiokawa et al. later (in 1990s) coupled the SAW with small droplet volumes to study phenomena like acoustic streaming flow, jetting, and atomization [14, 15]. Acoustic manipulation of small droplets (2003) and mixing using SAW-induced streaming flow (2006) were further elaborated with potential applications in biomedicine by Wixforth et al. using frequencies as high as 146 MHz [16, 17]. Friend and coworkers demonstrated ultrasonic atomization using a bulk acoustic waves (BAWs) device operated at 1.6 MHz, which highlights the contrast between the BAW- and SAW-based techniques [18]. These earlier works have led to discovery of interesting phenomena and exciting applications in recent years, e.g. unique finger instabilities (2012) and micro-centrifugation (2021) [19, 20].

1.2.3 History of Acoustic Radiation Force

On the other front, with King's [21] theoretical model of the "ARF" on a rigid spherical particle, a foundation was laid to calculate the force on a compressible droplet or bubble [22] or an elastic particle [23] exposed to a traveling or a standing acoustic wave. Gorkov's [24] simplified expression of the ARF model of Yosioka and Kawasima [22] is still a common reference for modern-day theoretical as well as experimental works on the subject. While the aforementioned theoretical models were being validated with corresponding experimental demonstrations of acoustic waves pushing on suspended particles in a fluidic media, it was not until 1993 that Mandralis and Feke [25] used the ARF to fractionate particles in a *continuous flow*. With the work of Coakley and coworkers [26] and Laurell and coworkers [27], a continuous acoustic manipulation of suspended particles was brought to the realm of microfluidics with the use of silicon-based microfabricated channels attached to a BAW transducer. Following suit, Huang et al. demonstrated standing SAW-based focusing (2008) [28] and separation (2009) [29] of microparticles in a continuous flow within a polydimethylsiloxane (PDMS) microchannel. Continuous separation of particles by a traveling SAW was demonstrated only in 2013 by Sung and coworkers [30] and Franke and coworkers [31] Over the past decades, the objects manipulated by the acoustic waves are getting smaller and smaller from cm-scale (1969) [23] elastic spheres to μm-scale (2004) [27] microparticles, droplets, and cells to nm-scale (2022) [32] nanoparticles, extracellular vesicles, etc. For further reading on the historical development of the field, readers may also refer to the following references: [2, 33].

1.3 What Is an Acoustic Wave?

1.3.1 Acoustic Parameters

An acoustic wave is an elastic wave where a medium is needed to carry disturbances within the displacement, velocity, and pressure fields to transfer energy from one point in space to another, where the medium properties play a critical role in regulating energy transport. Ripples on the surface of water, vibrations in a guitar string, and seismic activities resulting in earthquakes are examples of such waves. In contrast, inelastic electromagnetic waves do not depend upon any medium to carry the oscillating electric and magnetic fields to transport energy, and can propagate even in vacuum. For visualization of elastic waves, one can imagine a transverse wave on a vibrating rope in a sinusoidal shape, where one end of the rope is moving up and down while the other is tied to an anchor. The highest and lowest points on the rope are called the wave *crest* and *trough*, respectively. The peak-to-peak wave amplitude is measured vertically from crest to trough, whereas the wavelength is measured horizontally between adjacent crests or troughs (Figure 1.2). The number of crests (or troughs) passing by a specific point per second defines the wave frequency, which is directly related to the wavelength of a given waveform and the speed of that waveform propagating in the media. More specifically, the wave frequency equals the ratio of wave speed to wavelength. Some examples of waves propagating at very different frequencies and wavelengths within very different media include seismic waves (0.01–10 Hz) traveling through the earth, audible sound waves (20–20 000 Hz) traveling through the atmospheric air, and ultrasound (2–20 MHz) traveling through the body for biomedical imaging. In addition to the wave frequency, wave speed, and wavelength, other key parameters that are important to fully characterize an acoustic wave include particle displacement, particle velocity, absolute acoustic pressure, oscillating acoustic pressure, density fluctuations (as a result of oscillating pressure), acoustic attenuation, acoustic intensity and acoustic impedance. Since most of these parameters are interdependent, it is hard to manipulate one without affecting the others. For example, displacement, velocity, and pressure fields have the same waveforms with certain phase differences, where a variation in one field would directly alter the rest. Acoustic intensity, a measure of acoustic energy carried by a wave per unit area per unit time, is defined as the product of acoustic pressure and particle velocity. Similarly, acoustic impedance, a measure of the opposition a material offers to an acoustic wave propagation, is a product of the speed of sound and density of the medium.

1.3.2 Displacement, Velocity, and Pressure Fields

At the heart of acoustic wave propagation through a medium is the particle–particle interaction, where any particle of the medium transfers energy by simply interacting with its adjacent neighbor, triggering a displacement of the neighboring particle from its rest position. Although the acoustic wave causes local oscillations in the medium it travels through, the particles of the medium do not translocate with the

wave (Figure 1.2). The particles' to-and-fro displacement over time is represented by a time-dependent particle velocity field depicting the acoustic wave. Oscillation of these particles with a certain velocity field leads to periodic regions of compression (high pressure) and rarefaction (low pressure) within a medium, which constitute a periodic pressure field that is 90° out-of-phase with the displacement field [34]. The phase difference between the pressure field and velocity field is 0° or 180° depending upon the reference coordinates and direction of wave propagation. That means, in a traveling wave, the particles having the highest or the lowest displacement at any given point correspond to the pressure value of zero, and vice versa. A period of displacement, velocity, or pressure field containing exactly one compression and one rarefaction region forms one complete wavelength of the acoustic wave. It is worth noting that an increase in the acoustic pressure or the particle velocity would result in an increased intensity of the acoustic wave, as both of these parameters work in perfect synchrony.

1.3.3 Wave Propagation

Just like an optical beam of light, acoustic waves can also exhibit phenomenon like reflection, refraction, and transmission, where the mechanical properties of the media, e.g. density, compressibility, and speed of sound, play a pivotal role in acoustic wave propagation, in contrast to the important optical properties of media, e.g. refractive indices, for light wave propagation. At an interface between two media of different mechanical properties, i.e. acoustic impedances, a part of the incident acoustic wave is reflected back, and a part is transmitted across the interface (Figure 1.4). The angles, proportions, wavelengths (or frequencies), and velocities of the reflected and transmitted waves depend upon the relative acoustic properties of the two media. The angles and proportions will be decided by Snell's law and acoustic impedances of media, respectively. The acoustic wavelength across an interface would vary based on the relative acoustic wave velocity within the respective medium.

1.3.4 Wave Dissipation

Imagine an acoustic wave at 2 kHz frequency traveling from air (sound velocity of ~330 m/s) to water (~1500 m/s) (Figure 1.4). The acoustic wavelength would change

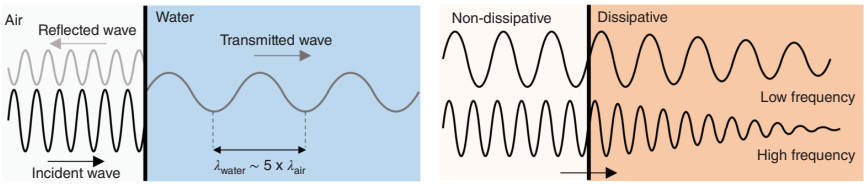

Figure 1.4 (left) Acoustic wave reflection and transmission at an air–water interface. (right) Transmission of an acoustic wave from a non-dissipative medium to a dissipative medium where the wave amplitude attenuates faster for high-frequency waves compared to low-frequency waves.

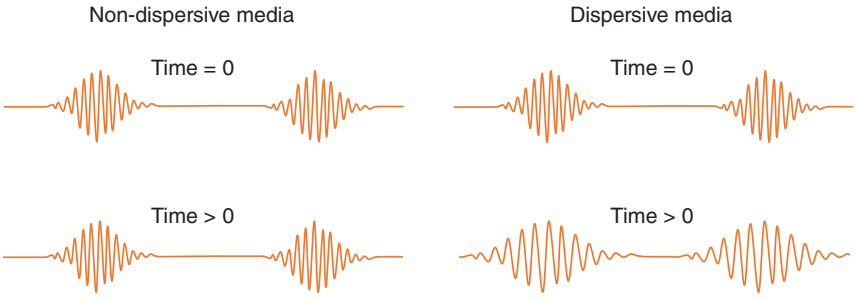

Figure 1.5 Nondispersive vs dispersive media.

from 165 to 750 mm across the air–water interface. A large portion of the wave amplitude will be reflected back into the air, and only a small portion will be transmitted into the water, which, in addition to ~5× longer wavelength, would make it extremely difficult to hear any sound underwater. Acoustic waves traveling through a viscoelastic dissipative medium such as water would also lose their energy due to viscous damping as the wave amplitude gradually attenuates over a length scale that is dependent on the acoustic wave frequency and medium viscosity (Figure 1.4). High-frequency waves attenuate faster in high-viscosity media, leading to shorter attenuation lengths, and vice versa. Since air viscosity is two orders of magnitude lower than that of water, it can sustain acoustic waves for longer distances for similar attenuation and frequency. Therefore, it is possible to hear low-frequency sounds through air over long distances compared to high-frequency sounds that dampen faster over short length scales.

1.3.5 Wave Dispersion

Acoustic wave velocity, or the speed of sound, stays constant for any range of frequencies in a nondispersive medium, but in a dispersive medium, it is frequency dependent (Figure 1.5). For instance, a sound waves packet composed of different frequencies can travel through the nondispersive media while maintaining a constant wave velocity for any given frequency and a consistent pulse shape over time. However, in a dispersive medium, high-frequency waves would travel faster than low-frequency waves; therefore, the acoustic pulse spreads out with time as it travels forward. The change in acoustic wave velocity is generally insignificant for most materials but not totally absent. For example, the speed of sound in air would increase by meager 0.1 m/s as the frequency is increased by an order of magnitude, i.e. <0.05% increment in the average speed of sound ~330 m/s.

1.4 Modes of Acoustic Waves

Acoustic waves can exist in several different modes, each with their own unique characteristics. They can be categorized based on the frequency range, wave propagation mode, or wave configuration.

1.4.1 Categorization Based on Frequency Range

Acoustic waves with frequencies in the audible range of 20 Hz to 20 kHz are known to human ears, which provides a good reference point to categorize the rest based on this frequency range (Figure 1.1). Low-frequency acoustic waves with frequencies below the audible range, i.e. <20 Hz, fall into the infrasound category. Avalanches, volcanoes, meteorites, and earthquakes are a few examples of infrasound-producing natural phenomena. Acoustic waves with frequency above the audible frequency range, i.e. >20 kHz, are usually referred to as ultrasound or ultrasonic. Ultrasonic waves are widely used in industrial settings, e.g. for cleaning parts located in difficult-to-reach regions where high-frequency acoustic waves remove the dirt, grease, and dust particles off the targeted surfaces. Moreover, ultrasonic waves have found a plethora of applications in biomedical sciences, including therapeutics, drug delivery and diagnostics (Figure 1.6). With their characteristic short wavelengths, ultrasonic waves imply a high degree of discrimination and a high concentration of energy; therefore, they can be used as a means of exploration, detection, actuation, etc. Starting beyond the audible frequency limit of 20 kHz, ultrasonic waves cover another three orders of magnitude higher frequencies beyond 10 MHz. These waves, with their broad range of frequencies, have been used for the improved delivery of drugs and genes to organs that are difficult to access, such as brain, for sono-dynamic and gene therapies, for thrombolysis and hemostasis, for healing bone fractures and treating osteoporosis, to mention a few. Acoustic waves having frequencies in GHz can be employed effectively in a variety of applications, including RF filters for 5G communication technologies, ultrawide band filters, and also in the components (such as actuators) of microelectromechanical systems. Bulk and SAW devices have been utilized at the RF front-end for a long time for filtering purposes where their operating frequencies are below 2.6 GHz range [36, 37]. Ultrasonic imaging, also known as ultrasound imaging or sonography, uses high-frequency sound waves to create images of the inside of the body. Also, ultrasonic sensors use sound waves at similar frequencies to measure distance, detect objects, and monitor fluid levels.

1.4.2 Categorization Based on Propagation Mode

Mechanical waves traveling at distances of 100s of kilometers during earthquakes to 10s of micrometers within microfluidic channels and miniaturized substrates demonstrate similar characteristics, which help in their categorization (Figure 1.7). Acoustic waves are categorized into following different types of waves based on particle movement in the medium and direction of wave propagation.

1.4.2.1 Longitudinal Waves

Longitudinal waves are the waves in which the particles of a medium vibrate in the same direction as the wave propagation. Material experiences periodic regions of compression and expansion as the waves travel forward (Figure 1.7). Longitudinal waves are also known as primary (P) compressional waves since they travel faster

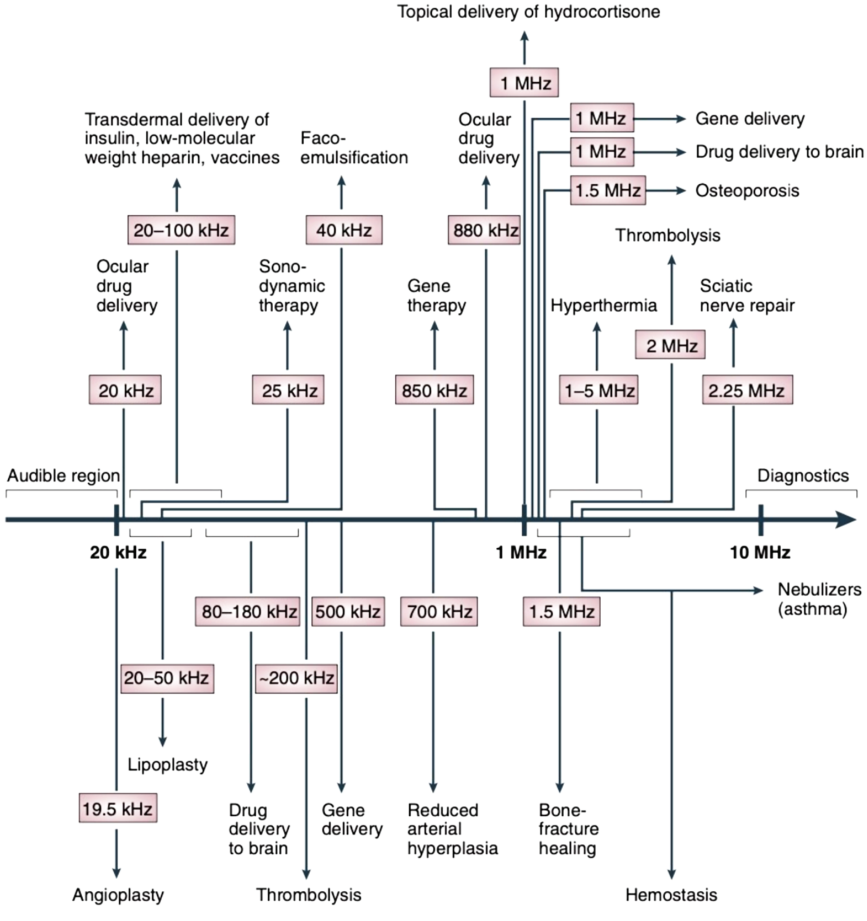

Figure 1.6 Summary of ultrasonic frequencies and their applications. Source: Reproduced from Mitragotri [35].

through the earth's crest than shear waves, which are also known as secondary (S) transverse waves (Figure 1.7a). A piezoelectric substrate sandwiched by a pair of electrodes can produce, on a much smaller scale, similar longitudinal or shear waves depending upon the orientation of piezo crystals, frequency of input current, thickness of the substrate, etc. (Figure 1.7b).

1.4.2.2 Shear Waves

Transverse or shear waves are waves in which the particles of a medium vibrate perpendicular to the direction of the wave propagation. This type of wave can propagate only in solids and not in liquids or gases since fluids cannot sustain a shear stress and only allow longitudinal waves to pass through. During an earthquake, the transverse S waves propagate with a velocity slower than the longitudinal P waves, arriving several seconds later than the longitudinal waves at

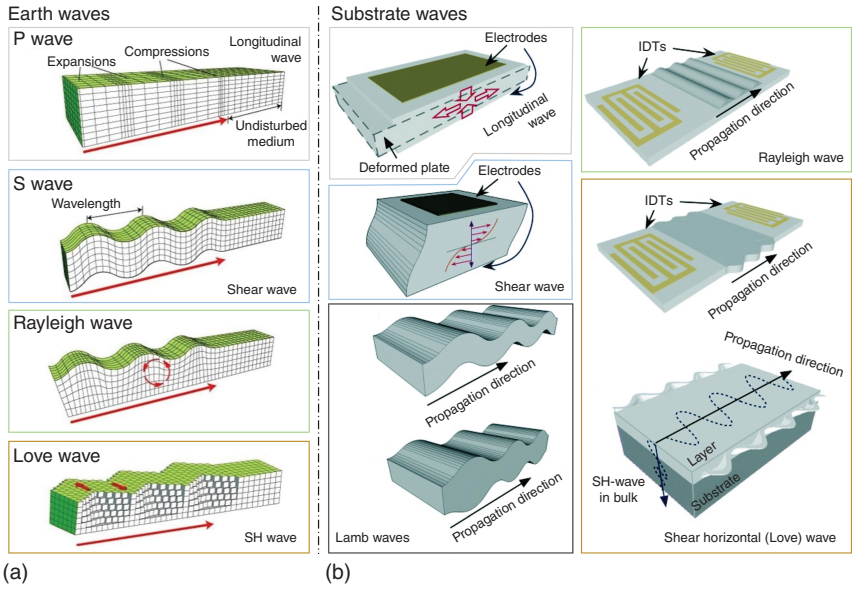

Figure 1.7 Categorization of waves based on propagation. (a) Propagation modes of earth waves. Source: Images courtesy: Copyright, Science Learning Hub - Pokapü Akoranga Pütaiao, University of Waikato [38]. (b) Wave propagation modes at a much smaller scale, i.e. within a substrate. Source: Fu et al. [39]/Reproduced with permission from Royal Society of Chemistry.

any given point. The same is true for a piezoelectric substrate, where longitudinal wave velocity is always greater than shear wave velocity.

1.4.2.3 Rayleigh Waves

Rayleigh waves, also known as surface waves, propagate across the surface of a medium where the particle displacements are both in the longitudinal and transverse directions. This renders a Rayleigh wave as a modal superposition of the longitudinal and shear waves. Due to these characteristics, the medium particles move in an elliptical orbit with velocity components parallel and normal to the wave propagation direction simultaneously. The amplitude of the particle displacement diminishes exponentially from the surface into the medium; therefore, the Rayleigh wave energy is mainly concentrated within a few wavelengths from the surface of the medium. These waves are mostly found in solids with wave velocity solely dependent on the material and the orientation of the crystals in the solid substrate. In liquids, a similar surface wave type is observed, i.e. water waves. However, the medium particles move in circular clockwise orbits in a rightward propagating water wave instead of elliptical orbits in Rayleigh wave, which switch from counterclockwise rotation to clockwise moving from the surface of a substrate to inwards of a substrate [34]. Rayleigh-type SAWs can be produced on specially oriented bulk piezoelectric substrates such as ST-cut and Y-cut quartz, 128° Y-X-cut lithium niobate ($LiNbO_3$), and X-112° Y-cut lithium tantalite ($LiTaO_3$) substrates.

Additionally, films made of zinc oxide, aluminum nitride, lead zirconate titanate, or $LiNbO_3$ that are vertically oriented (commonly referred to as *c*-plane or *z*-plane oriented) are also utilized to generate Rayleigh-type SAWs [39].

1.4.2.4 Love Waves

Love waves are horizontally polarized surface waves, which are named after Augustus Edward Hough Love, who first predicted them mathematically in 1911. These waves are responsible for horizontal shifting of the earth's crust during an earthquake and are only observed when the wave velocity in the upper layer is lower than the underlying sublayer. On a substrate, these shear-horizontal (SH) Love waves propagate through an isotropic thin layer sitting on a relatively thicker substrate and have a lower shear wave velocity compared to that of the substrate [40]. The isotropic layer on the substrate is usually much thinner than the wavelength of the SH Love waves, which are characterized by a unique horizontal shearing motion of the particles perpendicular to the direction of wave propagation and parallel to the device surface [39]. The SH Love waves can be produced on specially oriented bulk piezoelectric substrates, such as ST-cut quartz, 64° Y-X-cut $LiNbO_3$, and 36° Y-X-cut $LiTaO_3$.

1.4.2.5 Lamb Waves

Lamb waves are produced in a wave guide sandwiched between two parallel surfaces, such as the top and bottom surfaces of a plate or a substrate; therefore, they are also known as guided waves or plate waves [41]. The Lamb waves can propagate in a symmetric or an antisymmetric mode, where motion on the top surface is a mirror image of the bottom surface about the midplane of the plate or both surfaces are moving exactly in sync, respectively. Contrary to the Rayleigh waves, Lamb waves produce stresses throughout the plate thickness. The motion of any given particle within the plate vibrating in Lamb wave mode is always in the plane defined both by the surface normal and the wave propagation direction. The number of modes that each form of Lamb wave can achieve is unlimited. Frequency of the wave, angle of incidence, and material are some of the variables that affect the modes. The relation of frequency to wafer thickness determines the Lamb wave velocity. Because Lamb waves are extremely dispersive, their velocities change with frequency. Lamb waves can be used to solve a wide range of problems involving the identification of subsurface discontinuities for NDT since they can flow within thin plates.

1.4.3 Categorization Based on Wave Configuration

1.4.3.1 Traveling Waves

One can observe the crest of the wave moving along with the particles as it travels. After this crest, there is a trough, which is then followed by the next crest. In fact, one would identify a clear wave pattern moving through the medium in the shape of a sine wave. This sine wave pattern moves continuously until it encounters another wave in the same direction or until it changes the medium that have different property. This type of wave form that is observed traveling through a medium is described as a traveling wave (Figure 1.8).

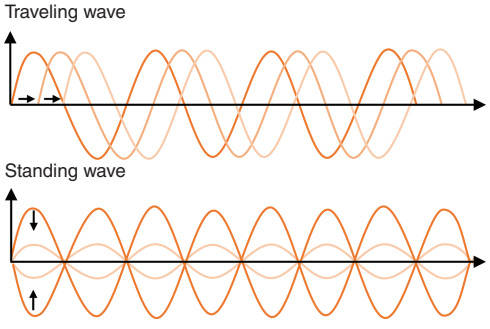

Figure 1.8 Traveling waves vs standing waves.

1.4.3.2 Standing Waves

Another type of wave pattern which is generated when reflected waves from one end of the medium interfere with incident waves from the source is defined as standing waves. Because of this interference, certain locations along the medium seem to be at a standstill. The pattern is commonly referred to as a standing wave pattern because the observed wave pattern is marked by points that appear to be standing still.

1.5 Acoustic Wave Propagation and Interaction

1.5.1 Transmission and Reflection of Acoustic Waves

When an acoustic wave encounters a boundary between two different media, a portion of the incident wave is reflected while the rest is transmitted through the boundary. The transmitted waves propagate through the interface from one medium to another, whereas the reflected waves remain in the same medium as the incident wave but propagate in the opposite direction. The ratio of the transmitted and reflected waves depends on the acoustic impedance values of the two media that form a boundary and the incident angle of the waves with reference to the normal to the boundary. The acoustic impedance (Z) of a medium is one of the fundamental physical properties of any medium and is defined as the product of its density (ρ) and its speed of sound (c), such that $Z = \rho c$. This specific property of the medium plays a crucial role in the reflection and transmission at boundaries between different media. When an acoustic wave travels from one medium with $Z_1 = \rho_1 c_1$ to another medium with $Z_2 = \rho_2 c_2$, the wave intensity and pressure amplitude of the incident, the transmitted and reflected waves, are determined by Z_1 and Z_2. The pressure transmission ($\boldsymbol{T}_P$) and reflection ($\boldsymbol{R}_P$) coefficients can be defined as the ratios of complex pressure amplitude of the transmitted ($\boldsymbol{P}_t$) and reflected ($\boldsymbol{P}_r$) waves to those of the incident wave ($\boldsymbol{P}_i$), such that $\boldsymbol{T}_P = \boldsymbol{P}_t/\boldsymbol{P}_i$ and $\boldsymbol{R}_P = \boldsymbol{P}_r/\boldsymbol{P}_i$, respectively. For harmonic plane traveling waves, the wave intensity (I) can be expressed as $P^2/2Z$, and the intensity transmission (T_I) and reflection (T_R) coefficients are defined as $T_I = (Z_1/Z_2)|\boldsymbol{T}_P|^2$ and $T_R = |\boldsymbol{R}_P|^2$, respectively [42, 43]. For oblique incidence of the waves with an incident angle of θ_i, the transmitted and reflected waves propagate at angles of θ_t and θ_r, respectively (Figure 1.9). The

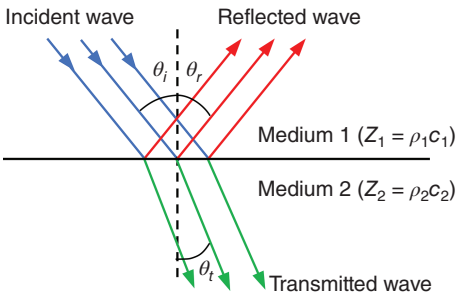

Figure 1.9 Wave reflection and transmission.

reflection and transmission of acoustic waves can be described mathematically using Snell's law, such that $\sin\theta_i/c_1 = \sin\theta_t/c_2$. The refraction angle, at which the transmitted waves travel through the new medium, is determined by the speeds of sound in two media and the incident angle (θ_i). Wave transmission and reflection play an important role in various applications, including acoustic imaging, which will be delineated in Chapters 4 and 5.

1.5.2 Acoustic Scattering

Acoustic scattering refers to the phenomenon in which the incident waves are redirected from the original propagation path when they encounter an obstacle that serves as a scatterer in the wave propagation process. The wave scattering phenomenon is influenced by many physical properties of the object and the acoustic wave, including size, shape, and acoustic properties of the object, and the frequency, amplitude, and polarization of the acoustic wave. Consider an object suspended in a fluid that is subject to an acoustic field, then the incoming waves are scattered off the object. A pressure field forms when vibration is introduced into a fluid medium. Three unique but interrelated scenarios result from the existence of an object in this vibrating medium: first, the interaction of the incident acoustic wave with the object; second, the scattering of the wave from the object; and third, the transmission of the wave into the object. These situations affect the pressure field based on the mechanical characteristics of the object placed in the wave path (i.e. size, shape, density, compressibility, and acoustic impedance). There is a net resultant force from these interactions with the acoustic waves, which is known as ARF. When wave scattering phenomena occur at solid–fluid interface, the wave exponentially decays while propagating in the fluid. In practice, this attenuation is comparatively small for solid–gas boundaries. The wave scattering phenomenon can be described by a nondimensional parameter called the Helmholtz number (ka), which is defined as the product of the wave number (k) and radius (a) when a spherical object (the scatterer) is placed at an infinitely large distance from it (in the far field), as shown in Figure 1.10a. The Helmholtz number can be interpreted as the nondimensional object size compared to the acoustic wavelength, and the three scattering regimes can be categorized depending on ka: Rayleigh scattering ($ka \ll 1$), Mie scattering ($ka \approx 1$), and geometrical scattering ($ka \gg 1$), as shown in Figure 1.10b. When the size of the object is much smaller than the wavelength

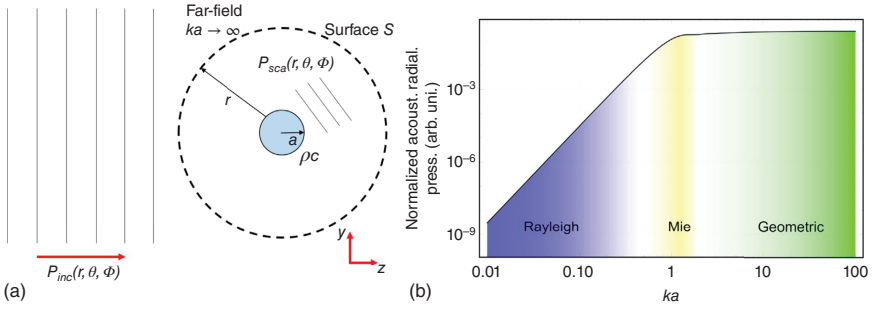

Figure 1.10 (a) Schematics of the acoustic scattering of an incident pressure field (P_{inc}) by a fluid sphere of radius (a), with internal (P_{int}) and external pressure (P_{Scat}) fields. (b) Representation of Rayleigh, Mie–like, and geometric scattering regimes when different values of the size factor ka for the air–water acoustic scattering were presented against normalized acoustic radiation pressure. Source: Pessôa and Neves [44]/Reproduced with permission from Elsevier.

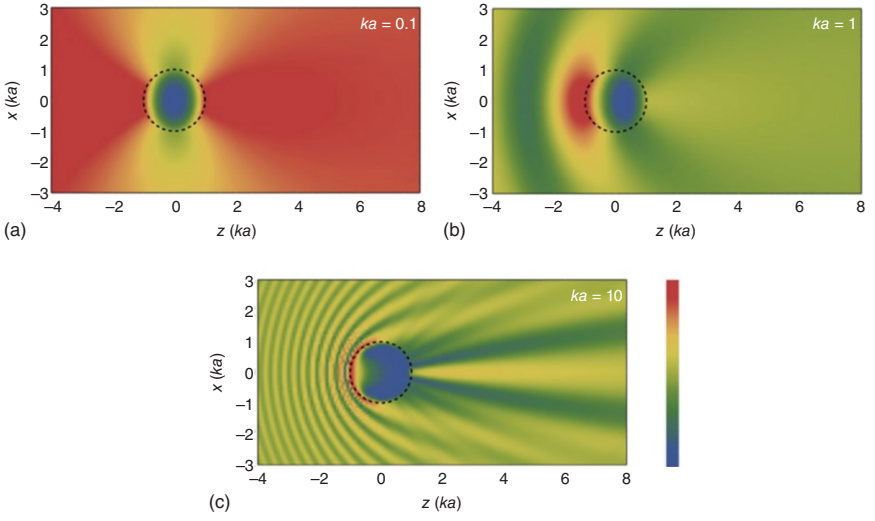

Figure 1.11 Total normalized pressure field. Scattering regimes for different *ka* values ($ka = 0.01$, $ka = 1$, and $ka = 10$). Source: Reproduced with permission from Pessôa and Neves [44], ELSEVIER.

(i.e. $ka < 1$) then the acoustic wave scattering is considered spherically isotropic scattering; however, when $ka \gg 1$, the scattering is no longer considered isotropic, and a net momentum transfer to the sphere occurs as backscattering dominates. The ARF can be assessed using a far-field examination of the scattering.

Figure 1.11 indicates an acoustic scattering of a water droplet of size factor *ka* in air. For small droplets with $ka = 0.01$, the scattering is in the Rayleigh regime, characterized by a minimum acoustic pressure intensity. For larger droplets with $ka = 1$, the scattering is in the Mie regime and can result in the formation of a high-pressure

intensity zone. For even larger droplets with $ka = 10$, the Mie scattering regime continues to be dominant.

1.5.3 Acoustic Radiation

ARF is a net force experienced by an object under the influence of an acoustic field. This force is caused by the transfer of wave momentum to scattering or absorbing objects due to an inhomogeneous wave scattering or reflection off the objects exposed to the acoustic field. At the interface, the acoustic wave can be partially reflected and transmitted, and these reflections and transmissions can contribute to originate the radiation force. The ARF can be discussed in two different ways depending on whether waves are traveling or standing. ARF on the object due to traveling acoustic waves is attributed to the anisotropic scattering of waves, but the force that arises due to standing acoustic waves is subject to the existence of pressure nodes and antinodes. When a solid sphere (elastic) is placed in the path of the wave, the force which is attributed to the scattering of the primary wave mainly depends on the resonant peaks at certain acoustic frequencies due to the free vibration of the spheres. More specifically, an inhomogeneous wave scattering occurs at the solid interface. On the other hand, when the fluid sphere (droplets and bubbles) is exposed to the acoustic scattering waves, the sphere suspended in the immiscible fluid experiences a distinct force due to the inhomogeneous geometrical wave scattering off the sphere. This force arises due to the mismatch in the acoustic impedances across the droplets/bubble interface with the surrounding fluid. The two components of ARF are the scattering component and the gradient component. The former component is directed toward wave propagation, but the direction of latter is perpendicular to wave propagation. The ARF in the Mie, Rayleigh, and geometrical scattering regimes varies by a number of factors, including the acoustic wave frequency, material properties of the scatterer, and the geometry of the object. The strength of the ARF is generally considered to increase in the order of Rayleigh scattering < Mie scattering < geometrical scattering regime. Rayleigh scattering occurs when the object size is much smaller than the wavelength of the acoustic wave, while Mie scattering occurs when the object size is comparable to the wavelength. In geometrical scattering, the object size is much larger than the wavelength, leading to a stronger ARF.

There has been much effort to investigate the ARF both experimentally and theoretically. Some of the milestone studies include King [21] and Maidanik [45] for rigid spheres, Hasegawa and Yosioka [23] and Tahmasebipour et al. [46] for elastic spheres, and Maidanik [45] and Yosioka and Kawasima [22] for fluid spheres. Interestingly, the most widely used polymer microspheres for biomedical applications, made of polystyrene (PS), polymethyl methacrylate (PMMA), polylactic acid (PLA), and polylactide-*co*-glycolide (PLGA), exhibit elastic behaviors when exposed to an acoustic field. The elastic microspheres experience an additional force that can be characterized by resonant peaks at certain acoustic frequencies due to the free vibration of the spheres [47, 48]. The available theories and their connections are summarized in Figure 1.12.

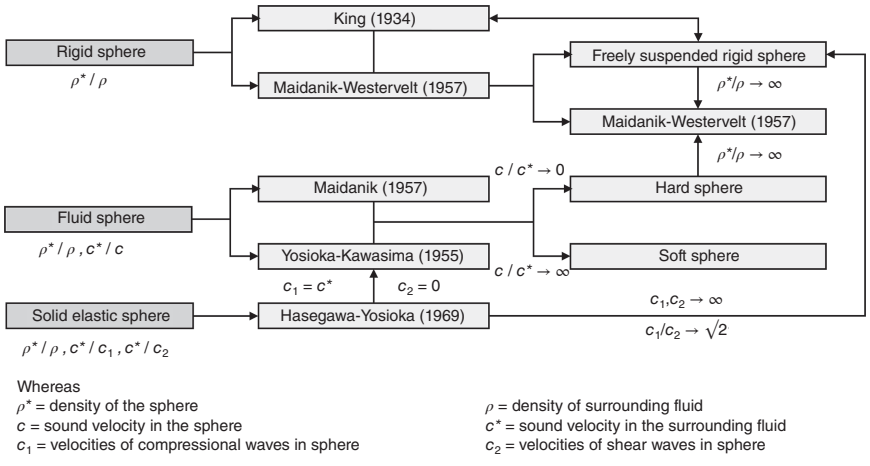

Figure 1.12 Different theories on wave scattering and their connection. Source: Hasegawa [49]/Reproduced with permission from Acoustical Society of America.

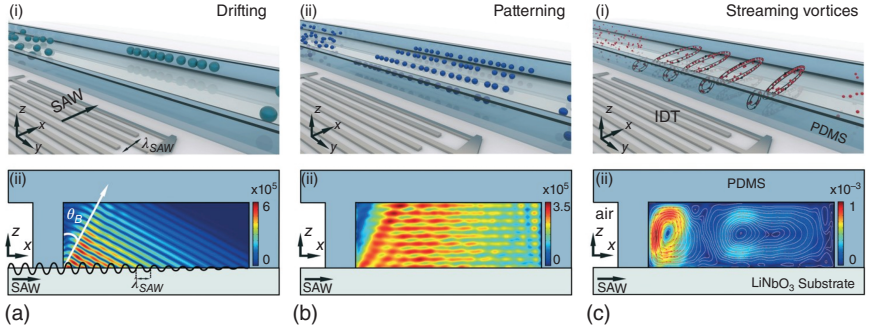

Figure 1.13 Migration, patterning, and swirling behavior of particles in the microfluidic channel. (a) particle drifting mechanism and illustration of acoustic wave propagation in the fluid. (b) particle patterning mechanism and simulated time-averaged absolute pressure field for particle patterning. (c) particle acoustic streaming flow mechanism and simulated streaming filed. Source: Fakhfouri et al. [50]/Reproduced with permission from Royal Society of Chemistry.

Acoustophoresis, defined as the manipulation of objects using acoustic forces, is widely utilized in various microfluidics applications such as manipulation of microparticles [47, 50], cells [51], droplets [52], and bubbles [53]. In a typical acoustically driven system, suspended objects are subject to steady-state acoustic forces that are generated by two main sources. Firstly, the presence of objects in a sound field causes scattering, which in turn produces ARF, which works to drive objects in a specific direction. Secondly, the resulting gradient of acoustic field provides a steady-state flow known as acoustic streaming flow (ASF). As soon as the wave reaches the edge of microfluidic microchannel, the wave refracted into the fluid domain within the microchannel in the form of longitudinal wave at the Rayleigh angle. The phenomenon of ASF results from gradients in the sound field as

it travels through a viscous fluid. These gradients cause time-averaged body forces to operate on the fluid. When the two mechanisms, ARF and ASF, arise within the fluid domain, the former give rise to the drifting (Figure 1.13a) and patterning (Figure 1.13b) of the suspended objects, whereas the latter give rise to the swirling behavior of the moving particles (Figure 1.13c) [50].

1.6 Acoustic Wave Attenuation

Loudspeakers in a cinema hall or a theater are not located only around the screen like miniaturized speakers in a cell phone or a tablet but distributed systematically throughout the large space to ensure uniform acoustic pressure for all the seats. This is to avoid uncomfortably high acoustic pressures for the front rows and diminished sound quality and intensity for the seats at the rear side of the hall. Nonuniform sound intensity in a large space can be explained by the attenuation of acoustic waves over long distances.

Attenuation or damping in a vibrating system can be defined as an irreversible reduction in amplitude of the oscillations. A dissipation of vibrational energy into thermal energy happens at the atomic scale, leading to a decay of acoustic wave amplitude at the macroscale. Understanding of a controlled dissipation of acoustic waves within a medium is essential to developing efficient materials. For example, materials with high attenuation coefficients are considered favorable for isolation of mechanical vibrations and noise in a system; conversely, for high-precision sensors and testing instruments, it is essential to maintain minimal damping of oscillating signals to gather measurements with high signal-to-noise ratio [54].

1.6.1 Viscoelastic Attenuation

Acoustic waves can attenuate by losing some of their amplitude at an interface due to reflection, transmission, or refraction of waves as described in Section 1.5.1. Moreover, a continuous attenuation of waves can occur within a medium due to intrinsic wave dissipation because of viscous, elastic, or viscoelastic losses. An elastic material under stress follows Hooke's law, i.e. deformation or strain in the material is directly proportional to the applied stress, and when the stress is removed, the strain also disappears without permanently altering the geometry of the material (Figure 1.14)

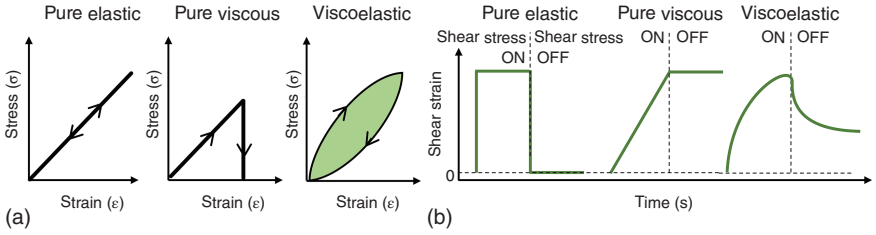

Figure 1.14 (a) Stress–strain diagram for elastic and viscoelastic materials. (b) Shear strain (compliance) over time under the applied shear stress to different material types.

[54]. In an ideal scenario, no energy is lost during the loading and unloading of the material. On the other hand, if the material is purely viscous, all the applied energy will be lost to the viscous dissipation and the shear strain will remain even when the applied stress is removed. Here, the stress–strain ratio determines the viscosity coefficient (μ) of the material, which means the viscous damping of acoustic waves would be higher in high-viscosity fluids. A combination of elastic and viscous behaviors is used to explain the viscoelastic materials, where some of the applied energy to induce strain will be lost during the material loading, and the material will return to its original shape with a hysteresis when the stress is removed. In every loading and unloading cycle, some of the vibration energy will be damped/absorbed by material.

1.6.2 Acousto-Thermal Heating

Under periodic stress in the form of high- frequency acoustic waves or vibrations, 10^3–10^6 of loading/unloading cycles per second can induce significant acousto-thermal heating of the viscoelastic material and high temperatures [54, 55]. The conversion of mechanical energy in ultrasonic waves to heat over time poses a critical challenge in systems where a constant temperature within the medium is essential to the intended operation. For example, viability of biological samples in the form of cells or proteins can be severely compromised within the acousto-microfluidic devices if the thermal energy produced during the acoustic wave dissipation is not timely removed using a constant fluidic flow or an active Peltier cooling element [56, 57]. However, in some cases, instead of actively removing acousto-thermal heating from the system, it can also be used to our advantage for various applications such as droplet sorting (marogami effect), thermochromic display and microheater/reactor [58–63].

1.6.3 Acoustic Streaming Flow

Propagation and attenuation of acoustic waves within a medium can lead to a bulk fluid flow, in the form of Eckart, Rayleigh, or bubble-driven streaming (Figure 1.15), with a non-zero average velocity that depends upon the transducer configuration, wave frequency, wave amplitude, dimensions of the fluidic domain, fluid viscosity, etc.

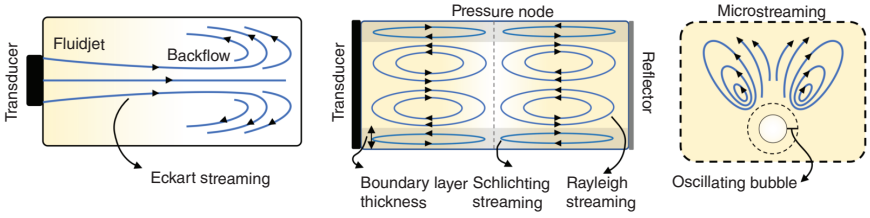

Figure 1.15 Acoustic streaming flows. Source: Wiklund et al. [64]/Reproduced with permission from Royal Society of Chemistry.

1.6.3.1 Eckart Streaming

Acoustic wave attenuation within a viscous fluid leads to a gradual reduction of the wave amplitude and formation of a pressure gradient in the direction of wave propagation, which generates a velocity field in the form of an acoustic streaming flow or Eckart streaming (Figure 1.15(left)) [12]. Eckart streaming is more pronounced when the attenuation length scale within the fluidic medium (L) is significantly larger than the acoustic wavelength (λ), i.e. $L \gg \lambda$. The attenuation length ($L \propto 1/\mu f^2$) is inversely proportional to the medium viscosity (μ) and acoustic frequency (f) squared. A single piezoelectric transducer, producing mainly traveling waves within a medium without significant wave reflection and standing wave formation, is ideal to generate Eckart streaming flow provided enough attenuation length is reached. Standing wave formation within the fluidic medium due to strong wave reflections at the boundaries could suppress the Eckart streaming flow. For example, a single 4 MHz ultrasonic transducer radiating traveling acoustic waves ($\lambda \approx 325$ μm) within a fluidic medium with maximum possible attenuation length of $L \approx 2$ mm (channel width, $L \gg \lambda$) produces Eckart streaming flow when the acoustic wave reflection from the planner PS reflector is minimal (Figure 1.16). However, when the waves are strongly reflected by a molybdenum reflector, they interfere with the incident traveling waves to form a standing acoustic field, which suppresses the Eckart streaming flow formation and concentrates the tracing particles at the standing waves pressure nodes.

1.6.3.2 Rayleigh Streaming

Rayleigh streaming flow is produced within standing waves resonators with acoustic pressure nodes and anti-nodes uniformly spaced at quarter wavelengths across the fluidic domain (Figure 1.15(center)). Due to the viscous attenuation at the boundaries of the acoustic resonator, a momentum flux between the node and anti-nodes of a standing wave results in an inner boundary layer flow also known as "Schlichting streaming" [11]. The Schlichting streaming, confined within a very thin boundary layer, triggers a Rayleigh streaming flow in the form of larger vortices spanning across the bulk of the medium (Figure 1.17) [10]. The boundary layer thickness

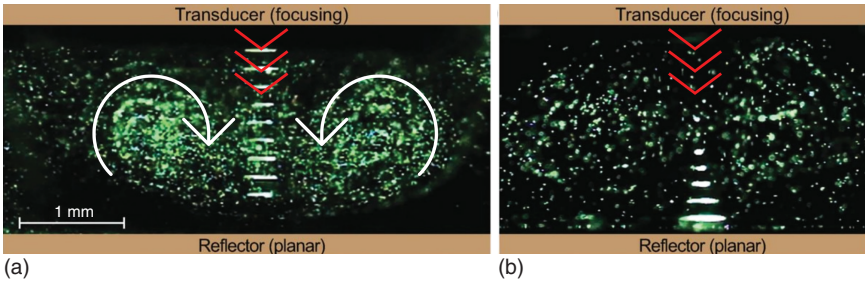

Figure 1.16 (a) Eckart streaming flow in the presence of weak wave reflector (polystyrene). (b) Streaming flow is suppressed, and standing waves are formed in the presence of a strong wave reflector (molybdenum). Source: Reproduced with permission from Wiklund et al. [64], Royal Society of Chemistry.

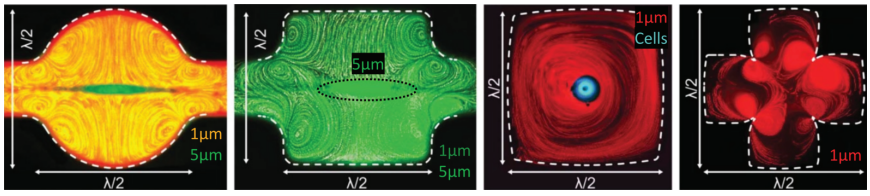

Figure 1.17 Rayleigh streaming patterns within standing wave resonators of different geometries. Source: Reproduced with permission from Wiklund et al. [64], Royal Society of Chemistry.

($\delta = \sqrt{\mu/\pi\rho f}$) provides a key reference dimension to identify Rayleigh streaming within a channel with characteristic length L; the following condition should hold to confirm the Rayleigh streaming flow: $\delta \ll L \ll \lambda$ [64]. For example, acoustic streaming patterns within standing wave resonators of different shapes ($L = \lambda/2$) can be easily traced with 1 μm microparticles, which move with the streaming flow contrary to the larger particles that are concentrated at the pressure nodes in the center due to the direct ARF (Figure 1.17). The boundary layer thickness (δ) for high-frequency O (MHz) acoustic waves is O (1 μm), which fulfills the condition $\delta \ll L(\lambda/2) \ll \lambda$ to confirm the Rayleigh streaming flow.

1.6.3.3 Bubble-Driven Microstreaming

Bubble-driven acoustic microstreaming occurs when a gas bubble trapped under in a liquid is subjected to high-frequency sound waves (Figure 1.15(right)). The bubble experiences a period of compression and rarefaction due to the alternating pressure of the acoustic waves, which forces the bubbles to decrease or expand in size, respectively. This cyclic expansion and contraction of the bubbles leads to the generation of localized flows or microstreaming around the bubbles. The resulting microstreaming depends on the frequency and amplitude of the acoustic waves, the size of the bubble, and the properties (density and viscosity) of the liquid surrounding the bubble. The frequency of the acoustic wave must be tuned for a strong actuation of the bubble for enhanced microstreaming generation, where the optimum frequency relates inversely with the bubble size. Bubble-driven acoustic microstreaming has found important applications in various fields, including microfluidics, drug delivery, and tissue engineering.

1.6.3.4 Applications of Acoustic Streaming Flow

Acoustic streaming flow has a variety of applications, including mixing and pumping fluids within microfluidic platforms, enhanced chemical processing in industrial reactors, cleaning labware, dental equipment and jewelry. For example, acoustic streaming is used to mix fluids within volumes that are difficult to mix otherwise [65]. Acoustic waves are further used to mix and manipulate even femtoliter-volume droplets within nanoslits in controllable manner [66]. Similar acoustic streaming effects have been used for particle or cell aggregation in sessile droplets [67–69]. Beyond acoustofluidic mixing of fluids, a high-power actuation of the sessile droplets could lead to jetting [70], translation [71], splitting [72], and atomization [73] of the

droplets. Within confined microchannels, active and rapid mixing of fluids in laminar flow regime [74, 75], sharp-edge and bubble-based acoustic streaming-induced mixing [76, 77] and pumping [78], nanoparticle focusing [79], and droplet pipetting or splitting [80] are other biomedical applications of the acoustic streaming flow. For more examples, the readers are encouraged to refer to the review articles by Connacher et al. [81] and Wu [82].

1.7 Generation and Propagation of Acoustic Waves

1.7.1 Acoustic Waves Generation in Nature

From communication to echolocation and from self-defense to preying on other animals, many living creatures in nature have evolved to generate and sense acoustic or sound waves of varying frequencies and intensities using only their bodily parts. For example, whales produce acoustic waves by moving air between their sinuses in the head, and they use oil-filled channel in their lower jaws to sense the reflected or echoed sound waves and conduct those to the middle ear for hearing (Figure 1.18a) [83]. Similarly, African elephants produce high-amplitude and low-frequency sound waves using their huge vocal cords. The infrasound travels through the ground and air to distant elephants, who hear it using their feet and ears in a way analogous to seeing and hearing lightning and thunder with a short delay time (Figure 1.18b) [84–86].

Similarly, we humans generate and sense sounds for communication, sharing feelings, expressing emotions by talking, singing, laughing, crying, screaming, shouting, humming, yelling, etc. Our bodies have evolved with an advanced mechanism, which incorporates three essential organs, lungs, vocal cords, and articulators, to perform these functions [87]. The lungs are working as a pump creating pressure to flow air through the trachea. Pressurized air flow vibrates the vocal folds to generate audible acoustic waves, where the pitch and tone of the waves can be adjusted by flexing the muscles of the larynx (epiglottis, supraglottic, vocal cord, etc.). The articulators above the larynx, such as tongue, palate, cheek, and lips, convert the sound waves produced by the vocal cords into speech or other sound expressions [88–90].

1.7.2 Generation of Acoustic Waves in Lab

1.7.2.1 Lower-Frequency Acoustic Waves

Acoustic waves are generated by any vibrating system such as vibrating strings of a guitar, diaphragm of a drum, and air within a resonant cavity of a flute. In industrial settings, vibrations are widely produced by an eccentric rotating mass (ERM)-based

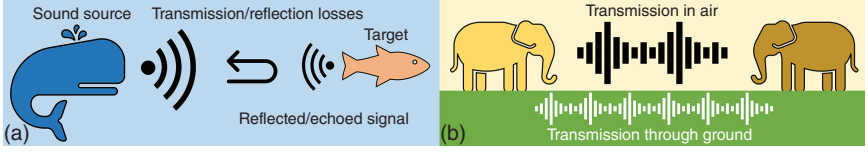

Figure 1.18 Echolocation examples for predator/prey (a) and elephant communication (b). Source: Adapted from Madsen and Surlykke [83].

DC (direct current) motor with an unbalanced mass placed on the motor shaft. Harmonic vibrations with tunable frequency and amplitude are generated by varying the angular speed and the offset of the ERM from the center of rotation. Alternatively, linear resonant actuators (LRAs) can generate an oscillating force across a single axis, resulting in low-frequency vibrations [91]. A moving mass with a "voice coil" wrapped around a magnet on one side and a "wave spring" on the other side for balancing oscillates under resonant-frequency AC excitation. The frequency and amplitude of the vibrations produced by LRA can be adjusted by changing the AC (alternative current) input. The vibrations coming out of the ERM- and LRA-based systems can be construed as acoustic waves with frequencies in hundreds of hertz. These vibratory systems are quite useful in haptic modules on mobile devices or for low-frequency manipulation of living objects by Faraday waves or ripples on a liquid-free surface. However, these low-frequency oscillators cannot generate ultrasonic waves required for most biomedical applications [92].

1.7.2.2 Piezoelectricity and High-Frequency Wave Generation

Since mechanical oscillators cannot reach ultrasonic frequencies, alternate methods have been sought after for decades, where a solution is found in piezoelectric materials to generate high-frequency acoustic waves. Piezoelectric ceramics can convert mechanical stresses (compression, tension, or shear) into electrical potential energy, and vice versa, without the need for any additional moving component. A voltage difference is produced across two electrodes sandwiching a piezo crystal going through a mechanical deformation due to the piezoelectric effect (Figure 1.19). Conversely, an applied voltage across those electrodes can deform the piezo crystal due to inverse piezoelectric effect. If the applied voltage potential is in the form of an alternating current of certain frequency, the deformation of the piezo element will turn in to oscillations of similar frequency. Since AC signals can be provided at a broad range of frequencies using a broad-range RF signal generator, piezoelectric elements can be made to oscillate and produce acoustic waves over several orders of magnitude frequencies (Hz–GHz). In addition to generating acoustic waves, piezoelectric or inverse piezoelectric effects can also be utilized for sensing or energy harvesting applications.

Piezoelectric materials have been used for a long time in a variety of fields such as acoustic detection of submarines [93], ultrasonic imaging of tissues, minimally invasive piezoelectric surgery [94, 95], industrial welding and cleaning by sandwiched

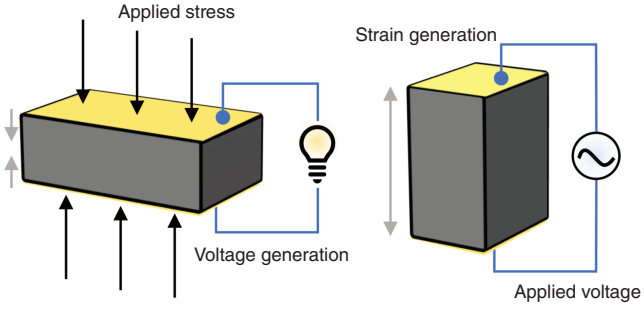

Figure 1.19 Two different ways of working principle for piezoelectric ceramics.

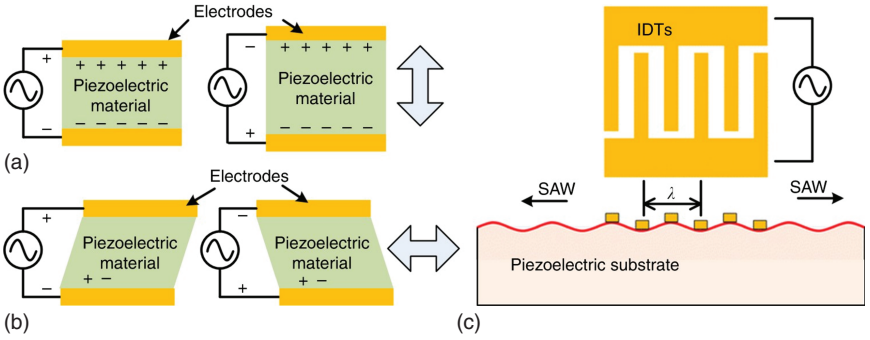

Figure 1.20 (a) Thickness mode vibrations. (b) Shear mode vibrations. (c) Surface acoustic waves (SAWs) produced by an interdigitated transducer (IDT). Source: Wu et al. [99]/Springer Nature/Licensed under CC BY 4.0.

Langevin-type high-power transducers [96], nondestructive and noncontact sensing [97], or energy harvesting system mobilized on movable devices to charge batteries [98]. Most of the early applications were based on BAW-based platforms for relatively low-frequency (kHz–MHz) requirements (Figure 1.20) [13]. The piezoelectric elements can be actuated by a thickness or shear-mode BAW depending on the crystal orientation, whereas the resonance frequency depends on the thickness of the element. It is possible to vibrate bulk of the piezoelectric element at very high frequencies and higher resonance modes; however, it is relatively less energy-efficient method. With the advent of interdigital transducers (IDTs), it became possible to generate acoustic waves at very high frequencies (MHz–GHz) in an energy-efficient manner. The IDTs are composed of thin-film metal electrodes placed periodically on the piezoelectric substrate surface and are able to generate high- frequency SAWs in an energy-efficient fashion as the waves are mainly concentrated at the surface of the substrate. SAW devices are extensively used in electronics industry for signal processing and cover a very broad band of frequencies from 10 MHz to 1 GHz. However, over past two decades, SAW devices have found themselves a new place in microfluidics to actively manipulate fluid and biological samples [100–103].

1.8 Acoustic Waves Effects in Fluidic Media

Acoustic waves in fluidic media can have a variety of effects depending on the frequency, amplitude, and the properties of the fluid. Some of these effects include acoustic streaming, mixing, sonication, cavitation, heating, atomization, and acoustic levitation. The acoustic waves in a fluidic medium can cause changes in the pressure of the fluid, which can be measured as sound pressure. At high frequencies and amplitudes, the acoustic waves can cause heating of the fluid, which can be used for therapeutic applications such as hyperthermia treatment for cancer [104]. The high-intensity acoustic waves can create bubbles in a fluid, which can collapse rapidly, generating high-pressure shocks and heat. This phenomenon, known as cavitation, can cause damage to materials and can be used for various

applications such as cleaning, mixing, and sonochemistry [105]. In microfluidic systems, acoustic streaming can be used to generate and control flow patterns, and manipulate particulate matters, including particles, cells, bubbles, and droplets. The acoustic techniques have been also widely utilized for lab-on-a-chip applications for cell sorting and separation, and chemical synthesis [106]. Acoustic waves can be used to levitate small particles and droplets in a fluid by producing an ARF [100]. This effect can be used for various applications, such as material processing and sample handling. Acoustic waves can also be used to mix fluids in laboratory applications by creating vortices and other flow patterns [107].

1.8.1 Vibrating Membranes and Sharp-Edge Structures

Upon submersion of specially made microstructures in the fluid, such as membrane and sharp-edge structures, and subjecting them to acoustic excitation, vortical flows or bubbles can be generated and controlled. The vibration of the microstructures creates pressure waves in the fluid, which can cause microscale fluid flows. The direction and magnitude of the flow can be controlled by manipulating the vibration frequency, amplitude, and geometry of the membrane or structure. Utilizing the vibrations of thin membranes and sharp-edged structures to produce acoustic streaming effects is a widely used method for controlling liquids and droplets in microfluidic systems. As explained in Section 1.6.3, acoustic streaming is a powerful tool for manipulating fluids and droplets at the microscale, where traditional fluid handling methods may not be feasible. The interaction between the acoustic wave and the fluid generates pressure variations that induce fluid motion in the form of acoustic streaming. The streaming effects utilizing these structures are dependent on the sharp-edge geometry, the frequency and amplitude of the applied signal, and the eigenmodes of the glass substrate. This streaming effect results in the formation of a localized vortex. Figure 1.21A,B shows an acoustofluidic device with sharp-edge structures that are utilized to achieve various flow operations. When the piezoelectric transducer is turned on, acoustic streaming patterns form at the tips of the oscillating sharp-edge structures. Figure 1.21C shows droplet manipulation via acoustic streaming generated by a vibrating membrane. Droplets can travel away from the membrane borders by using the vortex flow. Therefore, precise alignment of the membrane in relation to the streamlines results in the displacement of droplets from the edges of the membrane.

1.8.2 Oscillating Bubbles

Oscillating bubbles in microfluidics refer to the phenomenon of gas bubbles that periodically change in size and shape in a confined liquid environment. This is due to the interaction of the bubble with the liquid and the walls of the microfluidic channel. Oscillating bubbles can be generated by subjecting a fluid to a high-frequency vibration, which creates pressure waves in the fluid. These pressure waves can cause a bubble to form and begin to oscillate. The frequency, amplitude, and phase of the applied acoustic force can be used to control the oscillation of

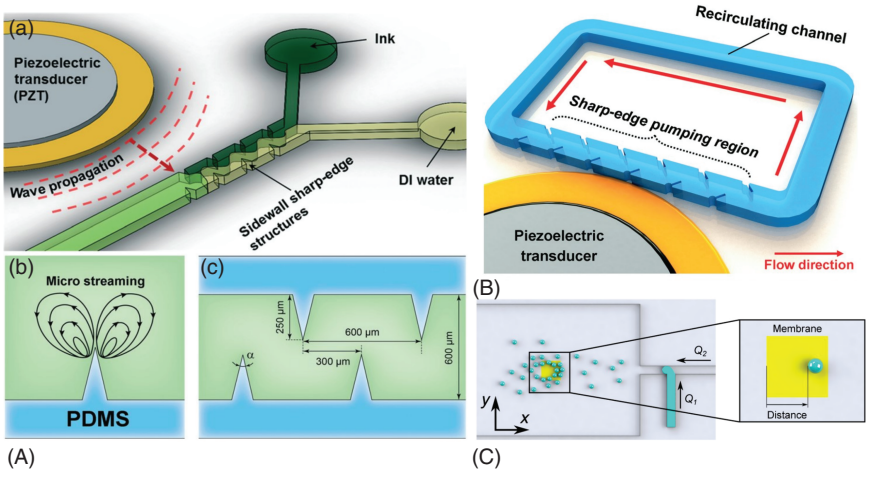

Figure 1.21 (A) Schematic of the sharp-edge-based acoustofluidic pumping device. Source: Nama et al. [108]/Reproduced with permissions from Royal Society of Chemistry. (B) Schematic of the device showing a microfluidic channel with sharp-edge structures on its side walls. Source: Huang et al. [109]/Reproduced with permissions from Royal Society of Chemistry. (C) Effects of the applied voltage on droplet repulsion from a single small membrane. Source: Reproduced with permission from Van Phan et al. [110] ©2016, American Chemical Society.

the bubbles. Oscillating bubbles have a wide range of applications in various fields. One of the most common is in sonochemistry, where the high-energy acoustic fields created by oscillating bubbles are used to promote chemical reactions. In the microfluidic platform, bubbles can be used to generate microstreams, which can be used for fluid mixing, particle manipulation, and droplet control [53]. Bubbles excited by an acoustic field act as an external energy source and induce a driving force at the interface between the bubbles and the surrounding liquid to induce vortical flows in the fluid. This phenomenon, also known as microstreaming, occurs when piezoelectric materials produce an acoustic wave by using an alternating current or radiofrequency. Generally, oscillating bubbles are a versatile tool that can be used to generate high-energy acoustic fields, which can be used to promote chemical reactions, control fluids and droplets, and manipulate particles.

1.8.2.1 Cavitation

Cavitation is becoming increasingly important in therapeutic ultrasonic procedures such as tumor ablation, lithotripsy, and diagnostics [105]. Cavitation refers to the formation and collapse of vapor-filled cavities, or bubbles, in a liquid that is subjected to changes in pressure. The development of bubble cavitation is caused by the rarefaction and compression cycles that an ultrasonic wave-induced pressure oscillation generates in the liquid. These vapor-filled cavities will collapse and produce a powerful shockwave in the form of a micro-jet when they are subjected to a substantially higher pressure; this phenomenon is known as inertial cavitation. In a wide range of industrial applications, ultrasonic cavitation effects can be used. Energy

produced by bubble collapse can be used to enhance the reaction rates of chemical processes, such as the solubilization of organic substances and the formation of free radicals [111]. Ultrasonic cavitation is occasionally combined with conventional stirring or other techniques in the production of biodiesel. Microalgae treatment as a feedstock for biodiesel also relies heavily on the mechanism of ultrasound cavitation. The ultrasonic frequency, ultrasonic source power intensity, fluid physical characteristics, initial bubble radius, and extra chemical reactions triggered during cavitation are the few variables that affect the efficiency of ultrasonic cavitation mechanism.

1.8.3 Optoacoustic Imaging

Optoacoustic imaging, also known as photoacoustic imaging or optoacoustic tomography (OAT), is a hybrid imaging technique that combines the high spatial resolution of optical imaging with the deep penetration of ultrasonic imaging. The basic principle of optoacoustic imaging is based on the photoacoustic effect, which is the generation of an acoustic wave in a material as a result of absorption of light. When a short pulse of laser light is absorbed by a biological tissue, it heats up and expands, creating an ultrasonic pressure wave that propagates through the tissue. In general, the optoacoustic technique is used to generate images of the internal structure of biological tissue by measuring the acoustic waves generated by the absorption of short pulses of laser light. Optoacoustic imaging can be used to image a wide range of biological tissues, including skin, breast, brain, and blood vessels. It has several advantages over traditional imaging techniques, including high spatial resolution, high contrast, and the ability to detect both optical absorption and scattering. The technology can be applied in various medical fields such as cancer detection and cardiovascular imaging [112]. When specific tissue components such as hemoglobin or lipids absorb this light, an ultrasound-induced mechanical wave is produced. These signals can be picked up by a transducer or transducer array, and can be transformed into images using different algorithms and other available techniques [112]. As depicted in Figure 1.22, the laser is used to deliver light to the sides of the transducer. Light is scattered by the tissue beneath the transducer array, and waves are produced using the transducer array. Photoacoustic imaging will be further delineated in Chapter 5.

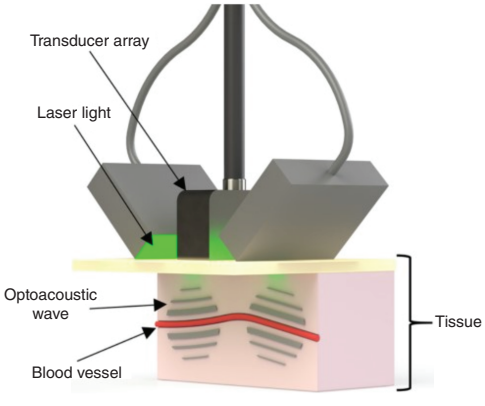

Figure 1.22 Schematic of optoacoustic imaging device. Source: Schellenberg and Hunt [113]/Reproduced with permission from Elsevier.

1.8.4 Manifestations of Acoustic Radiation Force and Acoustic Streaming Flow

ARF and acoustic streaming flow are two different phenomena that can be generated by an applied acoustic wave in a fluid. In microfluidics, these two phenomena are often observed simultaneously, where the ARF can be used to trap and manipulate micro-objects, while the acoustic streaming flow can be used to mix and transport fluids within the microchannel. The acoustic waves are typically applied using piezoelectric transducers or ultrasonic transducers that are placed near the microfluidic channel. The ability to manipulate micro-scale objects is crucial for a wide range of chemical and biological research. For the manipulation of small-scale objects, well-known traditional methods include centrifugation, sedimentation, and mechanical filtering. Later, various microfluidic systems were developed in which the use of optical, magnetic, dielectrophoretic and acoustic forces was of great interest. On-chip micro-object manipulations using acoustophoresis, typically at ultrasonic frequencies in the hundreds of kHz to tens of MHz range, have great potential to manipulate microscale objects. The microfluidic technology in the field of acoustophoresis is relatively straightforward to integrate within the systems. When an acoustic wave field is imposed on a microscale object suspended in the fluid, the former will be affected by ARF originating from wave scattering phenomena, as discussed in earlier section 1.5.3. In the case of BAW manipulation, acoustic waves spread through the bulk of a medium, whereas for SAWs-based devices, waves propagate along an elastic interface and transmit into the surrounding fluid medium. Besides the radiation forces, lateral acoustic streaming happens when an acoustic wave interacts with a fluid–fluid or solid–fluid interface, such as liquid drops in a gas or gas bubbles in a liquid and vibrating solid structure in the liquid. Further details on ARF and acoustic streaming flow can be found in Chapter 2.

List of Abbreviations and Symbols

radio frequency	RF
surface acoustic waves	SAWs
nondestructive testing	NDT
bulk acoustic waves	BAWs
acoustic radiation force	ARF
optoacoustic tomography	OAT
polydimethylsiloxane	PDMS
primary compressional waves	P-wave
secondary transverse waves	S-wave
lithium niobate	$LiNbO_3$
lithium tantalite	$LiTaO_3$
shear-horizontal Love waves	SH-wave
polystyrene	PS
polymethyl methacrylate	PMMA

polylactic acid	PLA
polylactide-*co*-glycolide	PLGA
acoustic streaming flow	ASF
order of magnitude	$O(\ldots)$
eccentric rotating mass based	ERM
direct current	DC
linear resonant actuators	LRA
alternative current	AC
interdigital transducers	IDT
acoustic impedance	Z
density	ρ
speed of sound	c
pressure transmission	$\boldsymbol{T}_P$
pressure reflection	$\boldsymbol{R}_P$
complex pressure amplitude of transmitted wave	$\boldsymbol{P}_t$
complex pressure amplitude of reflected wave	$\boldsymbol{P}_r$
incident angle	θ_i
reflected waves propagate angle	θ_r
wave number	k
spherical object radius	a
complex pressure amplitude of incident wave	P_i
internal pressure fields	P_{int}
external pressure fields	P_{Scat}
intensity transmission	T_I
intensity reflection	T_R
viscosity coefficient	μ
wave intensity	I
length scale within the fluidic medium	L
acoustic wavelength	λ
acoustic frequency	f
boundary layer thickness	δ

References

1 Ginsberg, J.H. (2018). *Acoustics – A Textbook for Engineers and Physicists*. New York: Springer.

2 Rossing, T.D. (ed.) (2007). *Springer Handbook of Acoustics*. Springer Science & Business Media.

3 Hirose, A. and Lonngren, K.E. (2010). *Fundamentals of Wave Phenomena*. IET.

4 Freegarde, T. (2012). *Introduction to the Physics of Waves*. Cambridge: Cambridge University Press. https://doi.org/10.1017/CBO9781139048149.

5 Lindsay, R.B. (1964). Report to the National Science Foundation on the conference on education in acoustics. *The Journal of the Acoustical Society of America* 36: 2241–2243.

6 Xiang, N. and Blauert, J. (2021). *Acoustics for Engineers*. Berlin: Springer.

7 Strutt, J.W. (1877). *The Theory of Sound*, vol. 1. Cambridge: Cambridge University Press. https://doi.org/10.1017/CBO9781139058087.

8 Faraday, M. (1831). XVII. On a peculiar class of acoustical figures; and on certain forms assumed by groups of particles upon vibrating elastic surfaces. *Philosophical Transactions of the Royal Society of London* 121: 299–340. https://doi.org/10.1098/rstl.1831.0018.

9 Dvořák, V. (1876). Ueber die akustische Anziehung und Abstossung. *Annalen der Physik* 42: 157.

10 Rayleigh, L. (1884). On the circulation of air observed in Kundt's tubes, and on some allied acoustical problems. *Philosophical Transactions of the Royal Society of London* 175: 1–21. http://www.jstor.org/stable/109434.

11 Schlichting, H. (1932). Berechnung ebener periodischer Grenzschichtstromungen. *Physikalische Zeit* 33: 327–335.

12 Eckart, C. (1948). Vortices and streams caused by sound waves. *Physical Review* 73 (1): 68–76. https://doi.org/10.1103/PhysRev.73.68.

13 White, R.M. and Voltmer, F.W. (1965). Direct piezoelectric coupling to surface elastic waves. *Applied Physics Letters* 7 (12): 314–316. https://doi.org/10.1063/1.1754276.

14 Shiokawa, S., Matsui, Y., and Ueda, T. (1990). Study on SAW streaming and its application to fluid devices. *Japanese Journal of Applied Physics* 29 (S1): 137. https://doi.org/10.7567/JJAPS.29S1.137.

15 Shiokawa, S. and Matsui, Y. (1994). The dynamics of SAW streaming and its application to fluid devices. *MRS Proceedings* 360: 53. https://doi.org/10.1557/PROC-360-53.

16 Wixforth, A. (2003). Acoustically driven planar microfluidics. *Superlattices and Microstructures* 33 (5, 6): 389–396. https://doi.org/10.1016/j.spmi.2004.02.015.

17 Sritharan, K., Strobl, C.J., Schneider, M.F. et al. (2006). Acoustic mixing at low Reynold's numbers. *Applied Physics Letters* 88 (5): 1–3. https://doi.org/10.1063/1.2171482.

18 Forde, G., Friend, J., and Williamson, T. (2006). Straightforward biodegradable nanoparticle generation through megahertz-order ultrasonic atomization. *Applied Physics Letters* 89 (6): https://doi.org/10.1063/1.2221914.

19 Rezk, A.R., Manor, O., Friend, J.R., and Yeo, L.Y. (2012). Unique fingering instabilities and soliton-like wave propagation in thin acoustowetting films. *Nature Communications* 3: 1167. https://doi.org/10.1038/ncomms2168.

20 Gu, Y., Chen, C., Mao, Z. et al. (2021). Acoustofluidic centrifuge for nanoparticle enrichment and separation. *Science Advances* 7 (1): eabc0467.

21 King, L.V. (1934). On the acoustic radiation pressure on spheres. *Proceedings of the Royal Society of London. Series A: Mathematical and Physical Sciences* 147 (861): 212–240. https://doi.org/10.1098/rspa.1934.0215.

22 Yosioka, K. and Kawasima, Y. (1955). Acoustic radiation pressure on a compressible sphere. *Acta Acustica united with Acustica* 5 (3): 167–173.

23 Hasegawa, T. and Yosioka, K. (1969). Acoustic-radiation force on a solid elastic sphere. *The Journal of the Acoustical Society of America* 46 (5B): 1139–1143. https://doi.org/10.1121/1.1911832.

24 Gorkov, L.P. (1962). On the forces acting on a small particle in an acoustic field in an ideal fluid. *Doklady Akademii Nauk SSSR* 6: 773–776.

25 Mandralis, Z.I. and Feke, D.L. (1993). Continuous suspension fractionation using acoustic and divided-flow fields. *Chemical Engineering Science* 48 (23): 3897–3905. https://doi.org/10.1016/0009-2509(93)80368-Z.

26 Harris, N.R., Hill, M., Beeby, S. et al. (2003). A silicon microfluidic ultrasonic separator. *Sensors and Actuators B: Chemical* 95 (1–3): 425–434. https://doi.org/10.1016/S0925-4005(03)00448-9.

27 Nilsson, A., Petersson, F., Jönsson, H., and Laurell, T. (2004). Acoustic control of suspended particles in micro fluidic chips. *Lab on a Chip* 4 (2): 131–135. https://doi.org/10.1039/b313493h.

28 Shi, J., Mao, X., Ahmed, D. et al. (2008). Focusing microparticles in a microfluidic channel with standing surface acoustic waves (SSAW). *Lab on a Chip* 8 (2): 221–223. https://doi.org/10.1039/b716321e.

29 Shi, J., Huang, H., Stratton, Z. et al. (2009). Continuous particle separation in a microfluidic channel via standing surface acoustic waves (SSAW). *Lab on a Chip* 9: 3354–3359. https://doi.org/10.1039/b915113c.

30 Destgeer, G., Lee, K.H., Jung, J.H. et al. (2013). Continuous separation of particles in a PDMS microfluidic channel via travelling surface acoustic waves (TSAW). *Lab on a Chip* 13 (21): 4210–4216. https://doi.org/10.1039/c3lc50451d.

31 Skowronek, V., Rambach, R.W., Schmid, L. et al. (2013). Particle deflection in a poly(dimethylsiloxane) microchannel using a propagating surface acoustic wave: size and frequency dependence. *Analytical Chemistry* 85 (20): 9955–9959. https://doi.org/10.1021/ac402607p.

32 Zhang, J., Chen, C., Becker, R. et al. (2022). A solution to the biophysical fractionation of extracellular vesicles: Acoustic Nanoscale Separation via Wave-pillar Excitation Resonance (ANSWER). *Science Advances* 8 (47): eade0640.

33 Augustsson, P. (2011). On microchannel acoustophoresis – experimental considerations and life science applications. http://lup.lub.lu.se/record/2203054/file/2203068.pdf.

34 Russell, D.A. (2022). Longitudinal and transverse wave motion. https://www.acs.psu.edu/drussell/Demos/waves/wavemotion.html (accessed 10 May 2022).

35 Mitragotri, S. (2005). Healing sound: the use of ultrasound in drug delivery and other therapeutic applications. *Nature Reviews. Drug Discovery* 4 (3): 255–260. https://doi.org/10.1038/nrd1662.

36 Zou, Y., Gao, C., Zhou, J. et al. (2022). Aluminum scandium nitride thin-film bulk acoustic resonators for 5G wideband applications. *Microsystems & Nanoengineering* 8 (1): 124. https://doi.org/10.1038/s41378-022-00457-0.

37 Dutta, J., Singh, A.V., Singhal, S., and Upadhayay, M.D. (2016). Design and simulation of a zinc oxide thin film bulk acoustic resonator filter for 2.6 GHz band applications. *IETE Journal of Research* 62 (1): 3–8. https://doi.org/10.1080/03772063.2015.1062734.

38 The University of Waikato (2007). Science Learning Hub, 21 July 2007. https://www.sciencelearn.org.nz/images/353-earth-waves (accessed 10 May 2023).

39 Fu, Y.Q., Pang, H.F., Torun, H. et al. (2021). Engineering inclined orientations of piezoelectric films for integrated acoustofluidics and lab-on-a-chip operated in liquid environments. *Lab on a Chip* 21 (2): 254–271. https://doi.org/10.1039/d0lc00887g.

40 Chen, M., Huan, Q., and Li, F. (2019). Excitation of moderate-frequency Love wave in a Plexiglas plate on aluminum semi-space. *The Journal of the Acoustical Society of America* 146 (6): EL482–EL488. https://doi.org/10.1121/1.5139192.

41 Su, Z. and Ye, L. (2009). *Identification of Damage Using Lamb Waves: From Fundamentals to Applications*. Springer Science & Business Media.

42 Kinsler, L.E. and Frey, A.R. (1950). *Fundamentals of Acoustics*. New York: Wiley.

43 Munoz Gutierrez, M.A., Prospero Sanchez, P.L., and do Vale Neto, J.V. (2005). An eigenpath underwater acoustic communication channel simulation. *IEEE Xplore* 1: 355–362.

44 Pessôa, M.A.S. and Neves, A.A.R. (2020). Acoustic scattering and forces on an arbitrarily sized fluid sphere by a general acoustic field. *Journal of Sound and Vibration* 479: 115373. https://doi.org/10.1016/j.jsv.2020.115373.

45 Maidanik, G. (1957). Acoustical radiation pressure due to incident plane progressive waves on spherical objects. *The Journal of the Acoustical Society of America* 29 (6): 738–742. https://doi.org/10.1121/1.1909032.

46 Tahmasebipour, A., Begley, M., and Meinhart, C. (2022). Acoustophoresis of a resonant elastic microparticle in a viscous fluid medium. *The Journal of the Acoustical Society of America* 151 (5): 3083–3093. https://doi.org/10.1121/10.0010418.

47 Destgeer, G., Jung, J.H., Park, J. et al. (2017). Acoustic impedance-based manipulation of elastic microspheres using travelling surface acoustic waves. *RSC Advances* 7 (36): 22524–22530. https://doi.org/10.1039/C7RA01168G.

48 Destgeer, G., Ha, B.H., Park, J. et al. (2015). Microchannel anechoic corner for size-selective separation and medium exchange via traveling surface acoustic waves. *Analytical Chemistry* 87 (9): 4627–4632. https://doi.org/10.1021/acs.analchem.5b00525.

49 Hasegawa, T. (1977). Comparison of two solutions for acoustic radiation pressure on a sphere. *The Journal of the Acoustical Society of America* 61 (6): 1445–1448. https://doi.org/10.1121/1.381460.

50 Fakhfouri, A., Devendran, C., Ahmed, A. et al. (2018). The size dependant behaviour of particles driven by a travelling surface acoustic wave (TSAW). *Lab on a Chip* 18 (24): 3926–3938. https://doi.org/10.1039/C8LC01155A.

51 Wang, K., Zhou, W., Lin, Z. et al. (2018). Sorting of tumour cells in a microfluidic device by multi-stage surface acoustic waves. *Sensors and Actuators B: Chemical* 258: 1174–1183. https://doi.org/10.1016/j.snb.2017.12.013.

52 Xi, H.-D., Zheng, H., Guo, W. et al. (2017). Active droplet sorting in microfluidics: a review. *Lab on a Chip* 17 (5): 751–771. https://doi.org/10.1039/C6LC01435F.

53 Li, Y., Liu, X., Huang, Q. et al. (2021). Bubbles in microfluidics: an all-purpose tool for micromanipulation. *Lab on a Chip* 21 (6): 1016–1035. https://doi.org/10.1039/D0LC01173H.

54 Akay, A. and Carcaterra, A. (2014). Damping mechanisms. In: *CISM International Centre for Mechanical Sciences, Courses and Lectures*, vol. 558, 259–299. Springer International Publishing. https://doi.org/10.1007/978-3-7091-1821-4_6.

55 Zener, C. (1940). Internal friction in solids. *Proceedings of the Physical Society* 52 (1): 152. https://doi.org/10.1088/0959-5309/52/1/322.

56 Augustsson, P., Barnkob, R., Wereley, S.T. et al. (2011). Automated and temperature-controlled micro-PIV measurements enabling long-term-stable microchannel acoustophoresis characterization. *Lab on a Chip* 11 (24): 4152–4164. https://doi.org/10.1039/c1lc20637k.

57 Mulvana, H., Cochran, S., and Hill, M. (2013). Ultrasound assisted particle and cell manipulation on-chip. *Advanced Drug Delivery Reviews* 65 (11, 12): 1600–1610. https://doi.org/10.1016/j.addr.2013.07.016.

58 Park, J., Jung, J.H., Destgeer, G. et al. (2017). Acoustothermal tweezer for droplet sorting in a disposable microfluidic chip. *Lab on a Chip* 17 (6): 1031–1040. https://doi.org/10.1039/c6lc01405d.

59 Park, J., Ha, B.H., Destgeer, G. et al. (2016). Spatiotemporally controllable acoustothermal heating and its application to disposable thermochromic displays. *RSC Advances* 6 (40): 33937–33944. https://doi.org/10.1039/c6ra04075f.

60 Cha, B., Kim, W., Yoon, G. et al. (2021). Enhanced solutal Marangoni flow using ultrasound-induced heating for rapid digital microfluidic mixing. *Frontiers of Physics* 9: https://doi.org/10.3389/fphy.2021.735651.

61 Ha, B.H., Lee, K.S., Destgeer, G. et al. (2015). Acoustothermal heating of polydimethylsiloxane microfluidic system. *Scientific Reports* 5 (1): 11851. https://doi.org/10.1038/srep11851.

62 COMSOL Multiphysics® (2022). *Generic 711 Coupler – An Occluded Ear-Canal Simulator*. Stockholm, Sweden: COMSOL AB.

63 COMSOL Multiphysics® (2022). *Theory of Thermoviscous Acoustics: Thermal and Viscous Losses*. Stockholm, Sweden: COMSOL AB.

64 Wiklund, M., Green, R., and Ohlin, M. (2012). Acoustofluidics 14: applications of acoustic streaming in microfluidic devices. *Lab on a Chip* 12 (14): 2438–2451. https://doi.org/10.1039/c2lc40203c.

65 Wixforth, A., Strobl, C., Gauer, C. et al. (2004). Acoustic manipulation of small droplets. *Analytical and Bioanalytical Chemistry* 379 (7, 8): 982–991. https://doi.org/10.1007/s00216-004-2693-z.

66 Miansari, M. and Friend, J.R. (2016). Acoustic nanofluidics via room-temperature lithium niobate bonding: a platform for actuation and

manipulation of nanoconfined fluids and particles. *Advanced Functional Materials* 26 (43): 7861–7872. https://doi.org/10.1002/adfm.201602425.

67 Li, H., Friend, J.R., and Yeo, L.Y. (2007). Surface acoustic wave concentration of particle and bioparticle suspensions. *Biomedical Microdevices* 9 (5): 647–656. https://doi.org/10.1007/s10544-007-9058-2.

68 Destgeer, G., Ha, B., Park, J., and Sung, H.J. (2016). Lamb wave-based acoustic radiation force-driven particle ring formation inside a sessile droplet. *Analytical Chemistry* 88 (7): 3976–3981. https://doi.org/10.1021/acs.analchem.6b00213.

69 Rezk, A.R., Yeo, L.Y., and Friend, J.R. (2014). Poloidal flow and toroidal particle ring formation in a sessile drop driven by megahertz order vibration. *Langmuir* 30 (36): 11243–11247. https://doi.org/10.1021/la502301f.

70 Tan, M.K., Friend, J.R., and Yeo, L.Y. (2009). Interfacial jetting phenomena induced by focused surface vibrations. *Physical Review Letters* 103 (2): https://doi.org/10.1103/PhysRevLett.103.024501.

71 Tan, M.K., Friend, J.R., and Yeo, L.Y. (2007). Microparticle collection and concentration via a miniature surface acoustic wave device. *Lab on a Chip* 7 (5): 618–625. https://doi.org/10.1039/b618044b.

72 Collignon, S., Friend, J., and Yeo, L. (2015). Planar microfluidic drop splitting and merging. *Lab on a Chip* 15 (8): 1942–1951. https://doi.org/10.1039/c4lc01453g.

73 Collins, D.J., Manor, O., Winkler, A. et al. (2012). Atomization off thin water films generated by high-frequency substrate wave vibrations. *Physical Review. E, Statistical, Nonlinear, and Soft Matter Physics* 86 (5): https://doi.org/10.1103/PhysRevE.86.056312.

74 Yaralioglu, G.G., Wygant, I.O., Marentis, T.C., and Khuri-Yakub, B.T. (2004). Ultrasonic mixing in microfluidic channels using integrated transducers. *Analytical Chemistry* 76 (13): 3694–3698. https://doi.org/10.1021/ac035220k.

75 Cui, W., Zhang, H., Zhang, H. et al. (2016). Localized ultrahigh frequency acoustic fields induced micro-vortices for submilliseconds microfluidic mixing. *Applied Physics Letters* 109 (25): 253503. https://doi.org/10.1063/1.4972484.

76 Ahmed, D., Mao, X., Shi, J. et al. (2009). A millisecond micromixer via single-bubble-based acoustic streaming. *Lab on a Chip* 9 (18): 2738–2741. https://doi.org/10.1039/b903687c.

77 Huang, P.H., Xie, Y., Ahmed, D. et al. (2013). An acoustofluidic micromixer based on oscillating sidewall sharp-edges. *Lab on a Chip* 13 (19): 3847–3852. https://doi.org/10.1039/c3lc50568e.

78 Fang, W.-F. and Lee, A.P. (2015). LCAT pump optimization for an integrated microfluidic droplet generator. *Microfluidics and Nanofluidics* 18: 1265–1275.

79 Collins, D.J., Ma, Z., Han, J., and Ai, Y. (2017). Continuous micro-vortex-based nanoparticle manipulation via focused surface acoustic waves. *Lab on a Chip* 17 (1): 91–103. https://doi.org/10.1039/C6LC01142J.

80 Sesen, M., Devendran, C., Malikides, S. et al. (2017). Surface acoustic wave enabled pipette on a chip. *Lab on a Chip* 17 (3): 438–447. https://doi.org/10.1039/c6lc01318j.

81 Connacher, W., Zhang, N., Huang, A. et al. (2018). Micro/nano acoustofluidics: materials, phenomena, design, devices, and applications. *Lab on a Chip* 18 (14): 1952–1996. https://doi.org/10.1039/c8lc00112j.

82 Wu, J. (2018). Acoustic streaming and its applications. *Fluids* 3 (4): 108. https://doi.org/10.3390/fluids3040108.

83 Madsen, P.T. and Surlykke, A. (2013). Functional convergence in bat and toothed whale biosonars. *Physiology* 28 (5): 276–283. https://doi.org/10.1152/physiol.00008.2013.

84 Günther, R.H., O'Connell-Rodwell, C.E., and Klemperer, S.L. (2004). Seismic waves from elephant vocalizations: a possible communication mode? *Geophysical Research Letters* 31 (11): https://doi.org/10.1029/2004GL019671.

85 O'Connell-Rodwell, C.E., Arnason, B.T., and Hart, L.A. (2000). Seismic properties of Asian elephant (*Elephas maximus*) vocalizations and locomotion. *The Journal of the Acoustical Society of America* 108 (6): 3066–3072. https://doi.org/10.1121/1.1323460.

86 Langbauer, W.R. (2000). Elephant communication. *Zoo Biology* 19 (5): 425–445. https://doi.org/10.1002/1098-2361(2000)19:5<425::AID-ZOO11>3.0.CO;2-A.

87 Mayo Clinic Staff (2023). Laryngitis, 22 June 2022. https://www.mayoclinic.org/diseases-conditions/laryngitis/symptoms-causes/syc-20374262 (accessed 10 May 2023).

88 Park, M.C. (2019). Understanding the multi-mass model and sound generation of vocal fold oscillation. *AIP Advances* 9 (10): https://doi.org/10.1063/1.5113911.

89 Stevens, K.N. (2000). *Acoustic Phonetics*. MIT Press.

90 Titze, I.R. (1994). *Principle of Voice Production*. Prentice Hall.

91 Precision Microdrive Using DC motors for energy harvest or LRAs for vibration detection. https://www.precisionmicrodrives.com/eccentric-rotating-mass-vibration-motors-erms (accessed 10 May 2023).

92 Guex, A.G., di Marzio, N., Eglin, D. et al. (2021). The waves that make the pattern: a review on acoustic manipulation in biomedical research. *Materials Today Bio* 10. https://doi.org/10.1016/j.mtbio.2021.100110.

93 Mason, W.P. (1981). Piezoelectricity, its history and applications. *Journal of the Acoustical Society of America* 70 (6): 1561–1566. https://doi.org/10.1121/1.387221.

94 Donald, I. (1974). *Sonar – The Story of an Experiment*. Pergamon Press.

95 Manbachi, A. and Cobbold, R.S.C. (2011). Development and application of piezoelectric materials for ultrasound generation and detection. *Ultrasound* 19 (4): 187–196. https://doi.org/10.1258/ult.2011.011027.

96 Rozenberg, L.D. (1973). The ultrasonic cleaning mechanism. In: *Physical Principles of Ultrasonic Technology* (ed. L.D. Rozenberg), 252–269. Boston, MA: Springer US. https://doi.org/10.1007/978-1-4684-8217-1_13.

97 Hellier, C.J. (2003). *Handbook of Nondestructive Evaluation*. McGraw Hill.

98 Saadon, S. and Sidek, O. (2011). A review of vibration-based MEMS piezoelectric energy harvesters. *Energy Conversion and Management* 52 (1): 500–504. https://doi.org/10.1016/j.enconman.2010.07.024.

99 Wu, M., Ozcelik, A., Rufo, J. et al. (2019). Acoustofluidic separation of cells and particles. In: *Microsystems and Nanoengineering*, vol. 5, no. 1. Nature Publishing Group https://doi.org/10.1038/s41378-019-0064-3.

100 Destgeer, G. and Sung, H.J. (2015). Recent advances in microfluidic actuation and micro-object manipulation via surface acoustic waves. *Lab on a Chip* 15 (13): 2722–2738. https://doi.org/10.1039/c5lc00265f.

101 Yeo, L.Y. and Friend, J.R. (2014). Surface acoustic wave microfluidics. *Annual Review of Fluid Mechanics* 46 (1): 379–406. https://doi.org/10.1146/annurev-fluid-010313-141418.

102 Ding, X., Li, P., Lin, S.C. et al. (2013). Surface acoustic wave microfluidics. *Lab on a Chip* 13 (18): 3626–3649. https://doi.org/10.1039/c3lc50361e.

103 Rufo, J., Cai, F., Friend, J. et al. (2022). Acoustofluidics for biomedical applications. *Nature Reviews Methods Primers* 2 (1): 30. https://doi.org/10.1038/s43586-022-00109-7.

104 Kok, H.P., Cressman, E.N., Ceelen, W. et al. (2020). Heating technology for malignant tumors: a review. *International Journal of Hyperthermia* 37 (1): 711–741. https://doi.org/10.1080/02656736.2020.1779357.

105 Hashmi, A., Yu, G., Reilly-Collette, M. et al. (2012). Oscillating bubbles: a versatile tool for lab on a chip applications. *Lab on a Chip* 12 (21): 4216–4227. https://doi.org/10.1039/C2LC40424A.

106 Wei, W., Wang, Y., Wang, Z., and Duan, X. (2023). Microscale acoustic streaming for biomedical and bioanalytical applications. *TrAC Trends in Analytical Chemistry* 116958. https://doi.org/10.1016/j.trac.2023.116958.

107 Li, Y., Cai, S., Shen, H. et al. (2022). Recent advances in acoustic microfluidics and its exemplary applications. *Biomicrofluidics* 16 (3): 031502. https://doi.org/10.1063/5.0089051.

108 Nama, N., Huang, P.-H., Huang, T.J., and Costanzo, F. (2014). Investigation of acoustic streaming patterns around oscillating sharp edges. *Lab on a Chip* 14 (15): 2824–2836. https://doi.org/10.1039/C4LC00191E.

109 Huang, P.-H., Nama, N., Mao, Z. et al. (2014). A reliable and programmable acoustofluidic pump powered by oscillating sharp-edge structures. *Lab on a Chip* 14 (22): 4319–4323. https://doi.org/10.1039/C4LC00806E.

110 Van Phan, H., Alan, T., and Neild, A. (2016). Droplet manipulation using acoustic streaming induced by a vibrating membrane. *Analytical Chemistry* 88 (11): 5696–5703. https://doi.org/10.1021/acs.analchem.5b04481.

111 Zheng, H., Zheng, Y., and Zhu, J. (2022). Recent developments in hydrodynamic cavitation reactors: cavitation mechanism, reactor design, and applications. *Engineering* https://doi.org/10.1016/j.eng.2022.04.027.

112 Karlas, A., Pleitez, M.A., Aguirre, J., and Ntziachristos, V. (2021). Optoacoustic imaging in endocrinology and metabolism. *Nature Reviews. Endocrinology* 17 (6): 323–335. https://doi.org/10.1038/s41574-021-00482-5.

113 Schellenberg, M.W. and Hunt, H.K. (2018). Hand-held optoacoustic imaging: a review. *Photoacoustics* 11: 14–27. https://doi.org/10.1016/j.pacs.2018.07.001.